THE ASTROPHYSICAL JOURNAL, 373:23–53, 1991 May 20

COMPARISONS OF THE EMISSION-LINE AND CONTINUUM PROPERTIES OF BROAD ABSORPTION LINE AND NORMAL QUASI-STELLAR OBJECTS[1,2]

RAY J. WEYMANN AND SIMON L. MORRIS
Observatories of the Carnegie Institution of Washington, 813 Santa Barbara Street, Pasadena, CA 91101
CRAIG B. FOLTZ
Multiple Mirror Telescope Observatory, University of Arizona, Tucson, AZ 85721
AND
PAUL C. HEWETT
Institute of Astronomy, Madingley Road, Cambridge CB3 0HA, England, UK
Received 1990 September 6; accepted 1990 November 1

ABSTRACT

We compare the emission-line and continuum properties of a set of 25 broad absorption line QSOs (BALQSOs) and 29 normal QSOs (i.e., non–BALQSOs), both taken from the Large Bright Quasar Survey (LBQS), whose candidates were identified using the Cambridge Automatic Plate Measuring Facility. The LBQS sample of 25 BALQSOs is augmented by an additional 17 BALQSOs taken from other sources. We define a *balnicity index* in order to separate the non–BALQSOs from the BALQSOs as objectively as possible, as well as to provide a measure of the strength of the broad absorption line features. The comparisons are made by defining indices for various features, measuring them for each object, and applying the Kolmogorov-Smirnov (K-S) test to various BALQSO and non–BALQSO samples. We also compare the BALQSOs and non–BALQSOs by creating and comparing mean spectra for various samples.

Our principal result is that *the emission-line properties of non–BALQSOs and BALQSOs are remarkably similar.* A comparison of the *LBQS* BALQSOs and non–BALQSOs reveals no statistically significant differences. However, when the *full* set of BALQSOs and various subsamples of the full set of BALQSOs are considered, we do find a small N V enhancement in the BALQSOs relative to the non–BALQSOs. We find enhanced emission around Al III λ1857, but comparison of the mean spectrum of the BALQSOs to the mean spectrum of the non–BALQSOs suggests that species other than Al III (probably Fe II and/or Fe III) are responsible for the difference. We also find a strong correlation between the strength of the Fe II emission and the balnicity index.

We define an index which measures the degree of detachment of the absorption trough. We find a weak anticorrelation between the detachment index and the equivalent widths of the C III] and C IV emission lines, but find no evidence of a correlation with this index and the Fe II strength. We confirm recent work by Corbin on velocity shifts between the peaks of Mg II, C III] and C IV: there is a small blueward displacement of the C IV peak relative to the C III] peak which is strongly correlated with the much larger blueward shift of C IV relative to Mg II. However, in contrast to Corbin's results, we do not find the shifts to be larger in the BALQSOs compared with the non–BALQSOs. There is evidence for structure in the C IV absorption troughs which has a velocity difference equal to that of the N V + Lyα velocity separation. This strongly suggests that radiation pressure is important in the dynamics of the outflow.

The continua of the BALQSOs and non–BALQSOs are remarkably similar, with the striking exception of the relatively rare BALQSOs which show strong Mg II and Al III absorption. These objects are much redder in the interval $\sim$1550 Å to $\sim$2200 Å than the other BALQSOs and non–BALQSOs. They also show especially strong Fe II emission, and evidence for Fe III emission much stronger than C III].

The close similarity between the emission-line and continuum properties of BALQSOs and non–BALQSOs is consistent with the view that BALQSOs do not form an intrinsically different class of objects from non–BALQSOs. We conclude that the small emission-line differences between non–BALQSOs and BALQSOs are more likely due to a difference in viewing angle, coupled with a mild anisotropy in the angular distribution of the flux of the emission lines, and a selection effect associated with a distribution of covering factors described by Morris. The Mg II–Al III BALQSOs may belong to an extreme population of objects where there is a large amount of obscuration present accompanying large, and therefore self-shielding, column densities, along with high electron densities.

Subject heading: quasars

[1] Some of the observations reported here were made at Palomar Observatory as part of a collaborative agreement between the California Institute of Technology and the Carnegie Institution of Washington.

[2] Some of the observations reported here were made with the Multiple Mirror Telescope, a facility operated jointly by the University of Arizona and the Smithsonian Institution.

I. INTRODUCTION

If one examines the Large Bright Quasar Survey (LBQS) sample of QSOs (which are optically selected to a limiting B_J magnitude of about 18.7) and considers those with redshifts above ~ 1.5, then the fraction which exhibit sufficiently strong blueward-displaced absorption in the C IV $\lambda 1549$ line to be placed in the broad absorption line (BAL) category of QSOs appears to be about 9%. When this fraction is corrected to take account of the depression of the flux in the B_J band caused by the absorption troughs, the fraction rises to about 12% (Foltz et al. 1990).

It has been realized for several years that this fraction could be interpreted in different ways: at one extreme one could suppose that there were two intrinsically different types of QSOs: a "non–BAL" type comprising about 88% of the QSOs and devoid of any BAL clouds, and the "BAL" type comprising the remaining 12%. In this view the absorbing clouds in the BAL type would have to cover most of the sky as seen from the center of the BALQSO. At the other extreme, one could imagine that all QSOs have broad absorption line regions with a covering factor having a small dispersion about a mean of 12%, with the 12% of the QSOs that we see as BALQSOs being those QSOs seen at the appropriate orientation. As noted by Morris (1988), however, it is far more likely that a variant of the latter view is correct—namely, that while essentially all radio-quiet[3] QSOs possess some high-velocity clouds causing the broad absorption troughs, there is a distribution in the covering factor over a fairly broad range.

It has also been realized for some time that a possible way of discriminating between these two views is to compare the properties of the emission lines in non–BALQSOs with those in BALQSOs. If indeed there are no intrinsic differences between the two types of QSOs and if the equivalent widths of the emission lines are not aspect-dependent, then one would expect no significant differences in the emission-line equivalent widths for the two classes of objects.

Several investigators have therefore carried out programs comparing properties of the broad emission line region (BELR) of BALQSOs and non–BALQSOs, e.g., Turnshek (1984b), Surdej & Hutsemekers (1987), Hartig & Baldwin (1986, hereafter HB), and Junkkarinen, Burbidge, & Smith (1987, hereafter JBS); see also Turnshek (1988) for the most recent general review of BALQSOs. Some of the results, as summarized recently by JBS, are as follows: (1) The Fe II emission is stronger in the BALQSOs by a factor of 1.5–3.0. (2) Al III $\lambda 1857$ emission is stronger in the BALQSOs by a factor of 1.5–3.0. (3) C IV $\lambda 1549$ emission is weaker in the BALQSOs by a factor of 0.3–0.6. (4) N V $\lambda 1240$ emission is stronger in the BALQSOs by a factor of 1.0–2.0.

There are several reasons for wishing to investigate this question further: (1) The sizes of both the BALQSO and non–BALQSO samples in these investigations have been fairly small, and our present sample adds significantly to the size of both samples and is in general of higher quality. (2) There is some disagreement between these investigators over the results summarized above—e.g., while all previous investigators have agreed that the N V/C IV ratio is higher in the BALQSOs than in the non–BALQSOs, HB conclude that this is primarily due to C IV being abnormally weak, while JBS and Turnshek conclude that N V is abnormally strong. (3) The non–BALQSO samples to date have included objects which differed considerably in absolute magnitude from the majority of the BALQSOs and included objects which were radio-loud sources, a property which the BALQSOs do not share (Weymann, Morris, & Anderson 1988). Since there are fairly strong luminosity effects in the properties of the BELR, and possibly subtler effects depending upon the radio properties as well (Baldwin, Wampler, & Gaskell 1989), it is important to choose the non–BALQSO objects from a sample which is optically selected in the same way as the BALQSO sample and which matches reasonably closely the luminosity of the BALQSO sample. (4) The BALQSOs differ widely in the strength and character of their absorption troughs, and these variations may well be correlated with some emission-line properties. It is possible that the "well-known" BALQSOs, most of which were discovered by visual inspection of objective-prism plates, are those with the strongest troughs and hence constitute in some sense a biased sample. We present evidence in support of this in § 4. (5) Finally, and most important, by defining and measuring quantitative indices as carefully as possible, one can hope not only to quantify the differences in these indices between samples (which is crucial for constructing models) but to assess the statistical significance of such differences as well.

The organization of this paper is as follows: In § 2 we describe how the objects were selected, the observational parameters characterizing the spectra, and the observation and reduction procedures. In § 3 we define a "balnicity index" (BI), which we use to segregate the non–BALQSOs from BALQSOs and provide a measure of the strength of the BAL features. We then define several measures of emission-line properties and present the results. In § 4 we define several subsamples of objects from our data set and carry out statistical tests to assess the reality of differences between the various subclasses. We also define a "detachment index" (DI) and examine the data set for correlations involving this index and the balnicity index. We then discuss the velocity shifts between the C IV, C III], and Mg II emission lines. In § 5 we carry out a comparison of the continuum properties, as well as further comparisons of the emission-line properties, by forming average spectra for several of the subsamples. Section 6 summarizes the results, and we discuss the conclusions we are able to draw.

2. OBJECT SELECTION, OBSERVATIONS, AND REDUCTIONS

2.1. *Object Selection*

The primary samples of BALQSOs and non–BALQSOs were drawn from the LBQS. An outline of the selection procedures and a preliminary account of the LBQS, the observations for which are now essentially complete, may be found in the first two installments of the survey (Foltz et al. 1987, 1989). A detailed discussion of the selection technique, along with a quantitative discussion of selection probabilities, is in preparation (Hewett et al. 1990). Direct CCD frames in B and V were taken at several positions over the field covered by each plate to yield B_J magnitudes accurate to ± 0.15 mag.

On the basis of comparisons with other selection techniques and with simulations, we believe that the LBQS QSOs, both the non–BALQSOs and the BALQSOs, are "free of selection

[3] Throughout this paper we use the terms "radio-loud," "intermediate," and "radio-quiet" QSOs. As a more precise working definition, we will consider objects with $\log R < 0.5$ to be radio-quiet, those with $0.5 \leq \log R \leq 2.5$ to be intermediate, and those with $\log R > 2.5$ to be radio-loud, where, following Kellermann et al. (1989), $\log R = \log F(6\text{ cm}) + 0.4 m_B - 6.66$ and where $F(6\text{ cm})$ is the 6 cm flux in millijanskys. For a QSO with $m_B = 18.0$, $\log R = 0.5$ corresponds to a flux of about 1 mJy.

effects" in the following sense: *Every object now known which is generally agreed to be a QSO, either a non-BALQSO or a BALQSO, and which has a redshift between 1.5 and 3.0 (to which interval the present study is restricted) would have a high probability of being found in the survey, regardless of the technique (radio, optical, X-ray, etc.) with which it was first found.*

All of the prominent emission lines from the N V + Lyα blend to the Mg II line are of interest in the comparisons of this paper, and it is desirable to measure, when possible, all these lines in the same object. For most of the spectra on which this work is based, the Hale Telescope with the Double Spectrograph (Oke & Gunn 1982) was used. In order to have adequate continuum longward of Mg II and shortward of Lyα to make meaningful measures of these emission features, the redshift range needs to be restricted to at least 1.90–2.20, with about 2.00–2.10 being optimum. Our observing lists for the non–BALQSO sample were therefore selected at random from a list of LBQS objects which had confirmed redshifts in this range and which did not appear to be BALQSOs on the basis of the relatively low signal-to-noise spectra of the LBQS candidates. (The majority of these identification spectra were MMT spectra, with the remainder taken with the Las Campanas du Pont Telescope.) Objects in the optimum range were given highest priority, consistent with availability in right ascension.

Unfortunately, the fraction of QSOs which are BALQSOs is so small that an insufficient number are available from our survey in this restricted redshift range. We therefore observed as many of the other LBQS BALQSOs as we could, which were known as of 1989 October, and whose redshifts were between 1.5 and 3.0, but with highest priority given to those in the optimum redshift range. Finally, we supplemented these BALQSOs with observations of known BALQSOs or BALQSO candidates from other sources. Section 4 discusses the formation of several statistical subsamples from all of these objects.

2.2. *Observations and Reductions*

As noted above, most of the data presented here were obtained using the Hale Telescope and Double Spectrograph utilizing a D52 dichroic filter. The red and blue detectors used were in both cases TI CCDs, with the blue side being oxygen-sensitized. The blue grating was a 300 grooves mm^{-1} first-order grating blazed at 3990 Å, and the red grating was a 158 grooves mm^{-1} grating blazed at 7500 Å, giving dispersions of 2.17 and 6.08 Å pixel, respectively. A 1″ slit was used which resulted in a FWHM resolution of about 6.5 Å in the blue and 18 Å in the red. The slit was oriented along the direction of atmospheric dispersion. Flux standards were observed each night. For the run of 1989 March 30–April 2 all the 1″ slit observations were preceded by short observations with an 8″ wide slit in an attempt to provide absolute fluxes and a calibration between flux and the LBQS B_J magnitudes.

The blue and red sides of the spectra were extracted, wavelength-calibrated, and reduced to a flux scale (and co-added when multiple exposures existed) following standard procedures and using the IRAF[4] reduction package. Atmospheric features were removed by division by a normalized early-type spectrum, but in many instances the air-mass match was not adequate to remove the A-band signature entirely. The red channel data were median-normalized so that the fluxes in the overlap region agreed, and rebinned to match the blue channel.

These spectra from the Hale Telescope were supplemented by observations in the red of other objects taken with the low-resolution cross-dispersed mode of the Red Channel Spectrograph of the MMT (Schmidt, Weymann, & Foltz 1989). These spectra covered the range ~4400 to ~9500 Å with a resolution of ~300 km s^{-1}. These red spectra were combined with blue spectra from several sources, including some observations from JBS.[5] The entire spectra of 0145+0416 (UM 139), 1333+2840 (RS 23), and 2225−0534 (PHL 5200) are those published by JBS. Information on the spectra for all of the objects discussed in this paper is summarized in Table 1.

Column (1) contains the usual coordinate designation for the object. Column (2) gives the source (e.g., "LBQS" or "known BALQSO"). Column (3) gives the source(s) for the spectra, while columns (4) and (5) give the approximate usable wavelength coverage and the date(s) of the observations. Column (6) gives the nominal redshift based upon a weighted mean of measurements of the peak wavelengths of Mg II, C III], and C IV, as discussed in § 4. The intrinsic luminosity of each object is of interest in connection with possible luminosity-dependent correlations of both spectral features and velocity shifts. Because the slit widths used in the observations were narrow, the derived fluxes, and hence luminosities, are subject to large uncertainties due to variations in seeing (as well as transparency) between the standard star and the program object observations. We have attempted to correct the observed fluxes to the values that would have been observed had all the observations been made with a wide slit, by multiplying the observed flux by a "flux factor." Column (7) gives this flux factor, and the letter following gives the basis on which the correction was made: "W" indicates it is based upon the small number of wide-slit (8″) observations described above which were obtained when conditions appeared to be photometric. "J" indicates that the flux factor was derived from the measured B_J magnitudes as follows: from the wide-slit observations of four LBQS objects which appeared to be taken under photometric conditions, we integrated the flux over the B_J-band sensitivity curve to establish the relation between this integral and the B_J magnitude. The narrow-slit fluxes for all the LBQS objects (which we believe to have reliable *relative* fluxes) were then integrated over the B_J-band instrumental response function, and the flux factor computed which yielded the B_J magnitudes actually measured from the calibrated direct plates. In the case of the known BALQSOs, no B_J magnitudes were available. "S" indicates that the flux factors are based upon unpublished Steward Observatory 90 inch (2.3 m) spectra taken with a wide slit under photometric conditions by Malkan, Rieke, & Weymann (1985). In a few cases we were obliged to simply use the fluxes derived from the narrow-slit observations of both the program objects and the standard stars, so that the flux factor is 1.00; we denote these cases by "N." In addition to the uncertainties inherent in these corrections, variability intrinsic to the QSOs may affect derivations of the flux factor where observations are separated by a substantial time interval.

Ideally, we would like to compare the bolometric luminosity of the objects, but, lacking any basis from which to estimate this, we defined a measure of the continuum brightness by

[4] IRAF is distributed by NOAO, which is operated by AURA, Inc., under contract to the NSF.

[5] We thank V. Junkkarinen for generously providing these spectra in digital form.

TABLE 1

OBJECT LIST AND OBSERVATIONAL PARAMETERS

object	obj src	spc src[a]	coverage	date obs	nom z	flx fct		log f	log L	other name	notes
0006+0230	LBQS	PAL	3410 9435	08.10.88	2.096	2.31	J	-16.06	43.28		
0009–0138	LBQS	PAL	3410 9445	08.09.88	1.999	1.48	J	-15.49	43.60		
0009–0215	LBQS	PAL	3410 9435	08.10.88	2.103	1.51	J	-16.17	42.99		
0010–0012	LBQS	PAL	3410 9420	08.09.88	2.160	1.40	J	-15.96	43.21		
0013–0029	LBQS	PAL	3410 9325	08.10.88	2.084	2.18	J	-16.08	43.23		
0019+0107	LBQS	PAL	3410 9415	08.09.88	2.123	1.14	S	-15.60	43.44	UM232	
0021–0213	LBQS	MMTB	3315 4490	09.09.88	2.293	1.00	J	-15.87	43.23		
		MMTR	4490 9885	10.23.89							
0025–0151	LBQS	MMTB	3230 4445	11.25.87	2.075	0.96	J	-15.67	43.28	UM253	
		MMTR	4445 9635	10.23.89							
0029+0017	LBQS	MMTB	3235 4430	11.25.87	2.229	1.33	J	-16.01	43.16		
		MMTR	4430 9880	10.23.89							
0043+0048	KNOWN BAL	LICK	3465 4450	08.17.79	2.146	1.00	N	-15.89	43.12	UM275	b
		MMTR	4450 9870	10.23.89							
0059–2735	LBQS	LCOB	3230 4835	08.31.89	1.593	1.88	J	-15.67	43.23		c
		LCOR	4835 9160	09.02.89							
0137–0153	KNOWN BAL	MMTR	4425 9900	10.23.89	2.234	1.00	N	-15.63	43.42	UM356	
0145+0416	KNOWN BAL	LICK	3405 8595	10.17.79	2.028	1.00	N	-16.03	42.90	UM139	b
0146+0142	KNOWN BAL	LICK	3630 4450	10.16.79	2.892	0.87	S	-15.70	43.63	UM141	b
		MMTR	4450 9840	10.23.89							
0226–1024	KNOWN BAL	MMTB	3270 4440	09.24.87	2.256	0.79	S	-15.16	43.81		
		MMTR	4440 9930	10.23.89							
0335–3339	KNOWN BAL	CTIO	3650 5090	12.10.85	2.258	1.00	N	-15.30	43.78		d
		LCOR	5090 9435	09.02.89							
0903+1734	KNOWN BAL	PAL	3375 9275	03.31.89	2.773	2.52	S	-15.95	43.79		
0932+5010	KNOWN BAL	PAL	3375 9275	03.30.89	1.911	3.12	S	-15.76	43.59		
1011+0910	KNOWN BAL	PAL	3375 9275	03.31.89	2.262	2.52	S	-15.90	43.57		
1029–0125	LBQS	PAL	3375 9275	03.30.89	2.036	3.20	J	-16.24	43.21		
1131+0114	LBQS	PAL	3400 9295	05.14.88	1.937	1.52	J	-15.87	43.19		
1139–0139	LBQS	PAL	3400 9285	05.13.88	1.960	1.53	J	-15.96	43.12		
1145+0121	LBQS	PAL	3375 9275	04.02.89	2.062	4.45	J	-16.47	43.14		
1146+0207	LBQS	PAL	3375 9275	03.31.89	2.055	2.96	W	-16.18	43.25		
1205+0918	LBQS	PAL	3375 9275	04.01.89	2.069	2.87	W	-16.07	43.35		
1205+1436	LBQS	PAL	3400 9280	05.12.88	1.632	2.60	J	-16.12	42.95		
1208+1535	LBQS	PAL	3400 9275	05.12.88	1.959	3.39	J	-16.15	43.28		
1212+1445	LBQS	PAL	3400 9250	05.12.88	1.626	1.84	J	-15.73	43.20		
1215+1527	LBQS	PAL	3400 9275	05.13.88	2.741	2.42	J	-16.36	43.34		
1216+1103	LBQS	PAL	3400 9250	05.13.88	1.616	1.34	J	-15.82	42.96		
1225+1512	LBQS	PAL	3375 9275	03.30.89	1.988	4.40	J	-16.30	43.25		
1227+1215	LBQS	PAL	3375 9275	04.02.89	2.166	2.64	W	-16.02	43.42		
1231+1320	LBQS	PAL	3400 9330	05.14.88	2.383	1.23	J	-15.72	43.51		
1232+1325	KNOWN BAL	PAL	3375 9275	04.02.89	2.361	2.31	W	-15.86	43.63		e
1234+0122	LBQS	PAL	3375 9275	03.30.89	2.024	3.42	J	-16.08	43.38		
1235+0857	LBQS	PAL	3500 9270	05.14.88	2.887	0.81	J	-15.68	43.62		
1235+1453	LBQS	PAL	3415 9265	05.14.88	2.686	2.08	J	-16.02	43.60		
1239+0955	LBQS	PAL	3400 9265	05.14.88	2.012	0.89	J	-15.62	43.26		
1240+1607	LBQS	PAL	3375 9300	03.30.89	2.357	4.78	J	-16.60	43.21		
1242+0006	LBQS	PAL	3375 9275	04.01.89	2.084	5.01	J	-16.17	43.50		
1243+0121	LBQS	PAL	3375 9275	03.31.89	2.790	3.15	J	-16.27	43.58		
1246–0542	KNOWN BAL	PAL	3375 9275	04.01.89	2.226	7.51	S	-15.97	43.97		
1303+3080	KNOWN BAL	PAL	3375 9275	03.30.89	1.763	2.39	S	-15.94	43.20	W22722	
1309–0560	KNOWN BAL	PAL	3375 9275	03.31.89	2.208	2.85	S	-15.91	43.60		
1314+0116	LBQS	PAL	3400 9265	05.14.88	2.693	1.35	J	-16.01	43.42		
1318–0150	LBQS	PAL	3375 9275	03.31.89	2.014	3.70	J	-16.42	43.08		
1323–0248	LBQS	PAL	3375 9275	04.01.89	2.123	6.67	J	-16.05	43.76		
1328+0223	LBQS	PAL	3375 9275	04.02.89	2.150	2.69	J	-16.42	43.02		
1331–0108	LBQS	PAL	3400 9260	05.14.88	1.874	1.61	J	-15.40	43.65		
1333+2840	KNOWN BAL	LICK	3305 8590	05.22.77	1.910	1.00	N	-15.72	43.14	RS23	b
1413+1143	KNOWN BAL	PAL	3375 9275	04.01.89	2.545	7.36	S	-16.19	43.91		
1428+0202	LBQS	PAL	3405 9265	05.14.88	2.109	1.43	J	-15.73	43.41		
1429–0053	LBQS	PAL	3375 9275	03.30.89	2.084	3.85	J	-16.13	43.43		
1433–0025	LBQS	PAL	3410 9195	08.10.88	2.047	2.28	J	-16.01	43.30		
1433+0223	LBQS	PAL	3375 9275	03.31.89	2.147	2.91	W	-16.19	43.28		
1439+0047	LBQS	PAL	3400 9290	05.14.88	1.857	1.69	J	-15.86	43.20		
1440–0024	LBQS	PAL	3400 9285	05.12.88	1.814	3.82	J	-16.12	43.26		
1442–0011	LBQS	PAL	3410 9240	05.13.88	2.216	1.98	J	-16.04	43.31		
1443+0141	LBQS	PAL	3400 9295	05.14.88	2.444	3.14	J	-16.13	43.54		

TABLE 1—*Continued*

object	obj src	spc src[a]	coverage	date obs	nom z	flx fct	log f	log L	other name	notes
1444–0112	LBQS	PAL	3375 9275	04.02.89	2.152	5.04 J	-16.45	43.27		
1641+4115	CC CAND	PAL	3375 9275	04.01.89	2.008	2.93 W	-16.67	42.73		e,f
2154–2005	LBQS	PAL	3415 9375	08.08.88	2.029	1.04 J	-15.71	43.24		
2201–1834	LBQS	LCOB	3230 4440	08.25.87	1.814	1.75 J	-15.51	43.53		
		MMTR	4440 9920	10.23.89						
2209–1842	LBQS	PAL	3420 9365	08.10.88	2.095	1.34 J	-15.77	43.34		
2211–1915	LBQS	PAL	3415 9390	08.09.88	1.951	1.00 J	-15.57	43.32		
2225–0534	KNOWN BAL	LICK	3405 8595	08.18.79	1.980	1.33 S	-15.80	43.23	PHL5200	b
2230+0232	LBQS	PAL	3415 9315	08.09.88	2.147	1.58 J	-15.91	43.30		
2244–0234	LBQS	PAL	3415 9365	08.08.88	1.966	1.60 J	-16.01	43.10		
2350–0045	LBQS	MMTB	3230 4440	09.29.89	1.624	1.41 J	-15.88	42.93		g
		MMTR	4440 9925	10.23.89						
2351+0120	LBQS	PAL	3420 9370	08.08.88	2.067	1.63 J	-15.98	43.19		
2356+0140	LBQS	PAL	3410 9315	08.09.88	2.067	1.15 J	-15.91	43.11		

[a] Sources for spectra: PAL = Hale Telescope Double Spectrograph; MMTB = Multiple Mirror Telescope Blue Channel Spectrograph; MMTR = Multiple Mirror Telescope Red Channel Spectrograph; Lick = Lick Observatory spectra from Junkkarinen et al. 1983, 1987; CTIO = CTIO 4 m unpublished spectrum from Turnshek et al. 1988; LCOB = Las Campanas du Pont Telescope with 2-D FRUTTI detector; LCOR = Las Campanas du Pont Telescope with modular spectrograph and CCD detector.

[b] The dates given for the Lick spectra refer to the last of a series of exposures. See Junkkarinen et al. 1983, 1987 for the journal of observations. The absolute flux scales for the narrow-slit observations are quite uncertain.

[c] Earlier LCOB exposure on 1988 September 12; blue spectrum of 1989 August 31 obtained with 4″ slit.

[d] Blue spectrum normalized to red spectrum taken with 2″ slit width under excellent seeing.

[e] Uncertain flux factor; possibly not photometric

[f] Cowley & Crampton 1987.

[g] This is object 2350−0045 Å in the list of Foltz et al. 1989.

selecting three windows having rest wavelengths in the region ~1975–2200 Å and then finding the median flux of all the pixels falling within any of these windows (see § 5). Column (8) gives the log of this monochromatic flux (in ergs cm^{-2} s^{-1} $Å^{-1}$) *before* multiplication by the flux factor. Column (9) gives the corresponding monochromatic luminosity (assuming $H_0 = 50$ and $q_0 = \frac{1}{2}$) based upon the fluxes in column (8), the flux factors in column (7), and the redshifts in column (6). Column (10) gives alternative names for the object, while column (11) provides notes or keys for explanatory notes at the bottom of the table.

In Figures 1*a*–1*l* we reproduce on a small scale the rest-frame spectra of all the objects in Table 1. When it was available we have also plotted the signal-to-noise ratio, calculated from the counting statistics associated with the object, sky, and detector noise.

3. DEFINITION OF BALQSOs AND EMISSION INDICES

3.1. *The "Balnicity Index"*

In most instances there is little doubt about whether a given QSO should be classified as a non–BALQSO or a BALQSO. Inevitably, there are borderline cases where it is not clear whether broad absorption is present or not, especially if the resolution and/or signal-to-noise ratio are not high. To remove as much subjectivity as possible and to provide a continuous rather than binary ("0 or 1") measure of "bal-ness," we have formulated a "balnicity index." The details of the formulation of this index, which follows the spirit of the working definition for BALQSOs proposed by Weymann, Carswell, & Smith (1981) are presented in Appendix A, but the essence is as follows: the index (which is to be applied to C IV) measures the equivalent width of strong absorption features (expressed in km s^{-1}) but requires that each absorption feature contributing to the index span at least 2000 km s^{-1}. We require this in order to exclude intervening systems. In addition, we exclude the first 3000 km s^{-1} blueward of the emission peak to distinguish the strong "associated absorption" from the broad absorption, since these two types of absorption appear to be quite different phenomena (Foltz et al. 1986).

Objects which have very weak and/or sharp absorption features have balnicity index of zero, while objects which are treated as BALQSOs in this paper have indices which are greater than zero and in principal could have a maximum value of 20,000 km s^{-1}. We have applied the algorithm described in Appendix A to all the objects in Table 1. In general, the results are in accord with our previous classification of the objects as BALQSOs or non–BALQSOs based on visual inspection of the spectra. An exception to this is the object 0302+170 (Foltz et al. 1985), which in the past has been considered a BALQSO. Most of the absorption in this object is contained within 3000 km s^{-1} of the emission peak and therefore does not contribute to the balnicity index. This object was therefore not included in our sample of BALQSOs or of non–BALQSOs, since we have restricted the non–BALQSO sample to the LBQS objects.

In Table 2 we list in column (1) the object name and in column (3) the balnicity index. We have split the table vertically into (3) sections: the top section contains those objects (all from the LBQS survey) which have a balnicity index of zero. Inspection of the spectra (see Fig. 1) of the objects contained in this section of Table 2 confirms that none of these objects are BALQSOs. The bottom section of Table 2 contains objects which are almost certainly true BALQSOs, although for the few with balnicity indices under 1500 km s^{-1} we may be seeing some cases of absorption, such as those associated with GC 1556 (Morris et al. 1986) or with the pair Tol 1037, 1038 (Jakobsen et al. 1986; Sargent 1988), which appear to involve exceptionally strong intervening complexes.

The two objects in the middle section of the table are obvi-

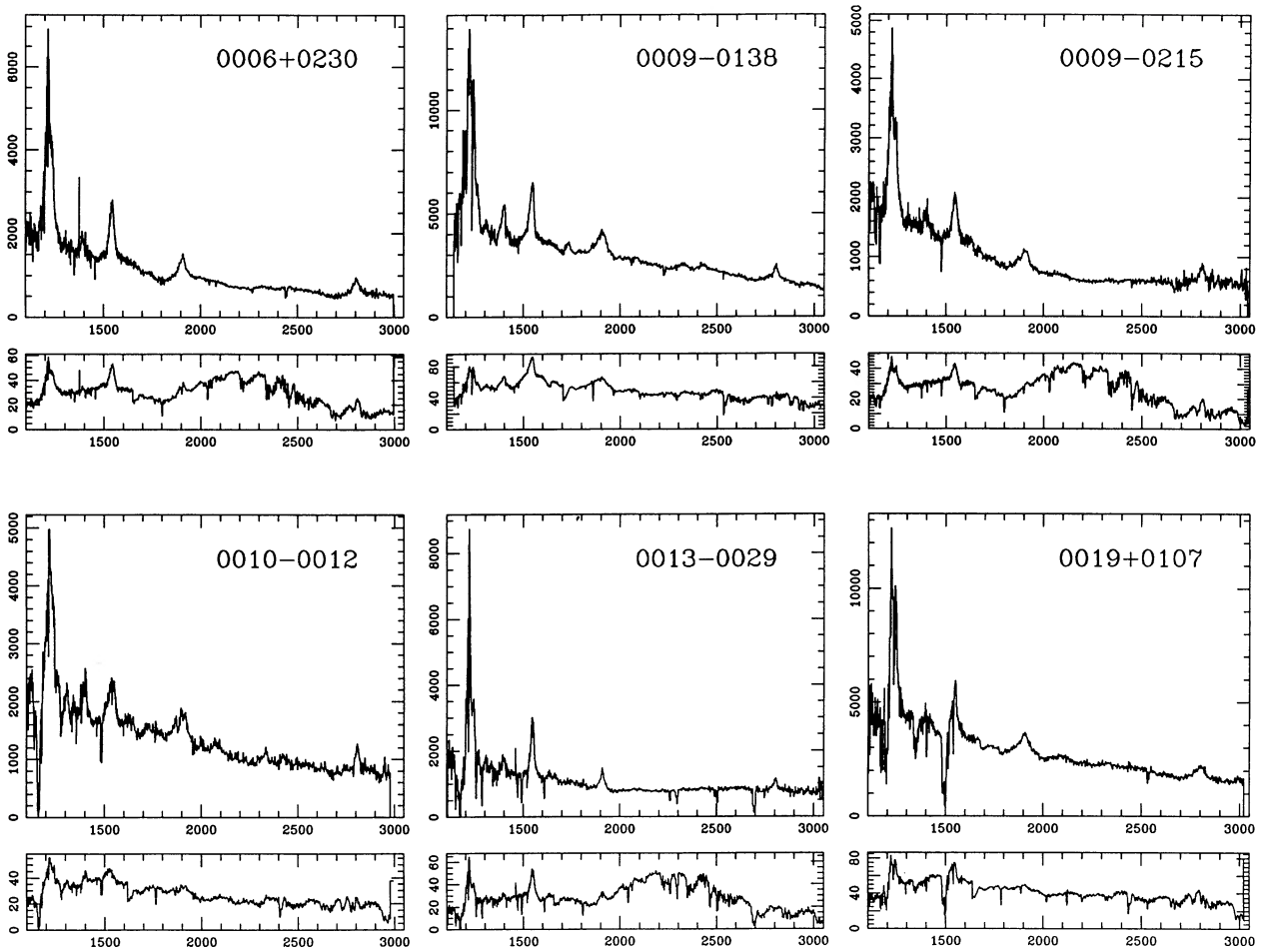

FIG. 1a

FIG. 1.—(*a–l*) Spectra of all 71 objects in the sample (*upper panels*). The objects have been redshifted to their rest frames as described in the text. The ordinate for the upper panels is the luminosity (in units of 10^{40} ergs s^{-1} $Å^{-1}$) calculated assuming $H_0 = 50$ and $q_0 = 0.5$. The lower panels represent the signal-to-noise ratio per pixel, when available, calculated from the counting statistics associated with the object, sky, and detector noise.

ously marginal cases, as is evident from the balnicity indices, which are just barely above zero. In the case of 1234+0122 we are almost certainly seeing an intervening absorption complex. As noted in Appendix A, it is appropriate to remove those absorption features which can be identified with species other than C IV (see also Appendix C), but our data are not of adequate resolution to do this reliably. The case of 2211−1915 is more doubtful. We consider it probable that it too involves intervening absorption, but better resolution data, coupled with a more refined definition of balnicity, are required to treat such borderline cases. Pending this, in our statistical treatments in § 4 we run parallel tests in which these two objects are treated as belonging to either the non–BALQSO or the BALQSO samples, but we have generally treated them as non–BALQSOs.

3.2. *Emission-Line Indices*

We now define several emission-line indices whose distributions we want to examine for differences between the non–BALQSO and the BALQSO samples or whose correlation properties we wish to study. It should be emphasized that it is not necessary that these indices measure *precisely* what they are nominally intended to measure. Our objective is to quantify any measurable differences in emission-line properties between the BALQSOs and the non–BALQSOs using indices which are as free of the effects of the absorption itself and as free of subjectivity as is practicable. With this understanding we have measured the following indices of line strength.

3.2.1. *Strength of the* N V λ1240 + Lyα *Blend*

We believe that the complexity of the region of the N V + Lyα blend in the BALQSOs makes it risky to attempt to deconvolve these two lines. It also makes an accurate location of the N V peak difficult. We have therefore proceeded as follows: (*a*) Fit a rough continuum to the spectrum with a low-order polynomial so that the resultant spectrum is approximately flat. (*b*) Define (rather than measure) the location of the N V peak by assuming it is located at a wavelength given by $\lambda_{\mathrm{N\,V\,peak}} = \lambda_{\mathrm{C\,IV\,peak}} \times 1240.1/1549.0$, i.e., assume that there is no velocity shift between the C IV and N V peaks. (*c*) Redraw a local continuum in the region of the spectrum redward of the N V peak to about 1300 Å. *The uncertainty in how to define this local continuum for the strong BALQSOs introduces a substantial uncertainty in this index.* (*d*) Measure the equivalent width

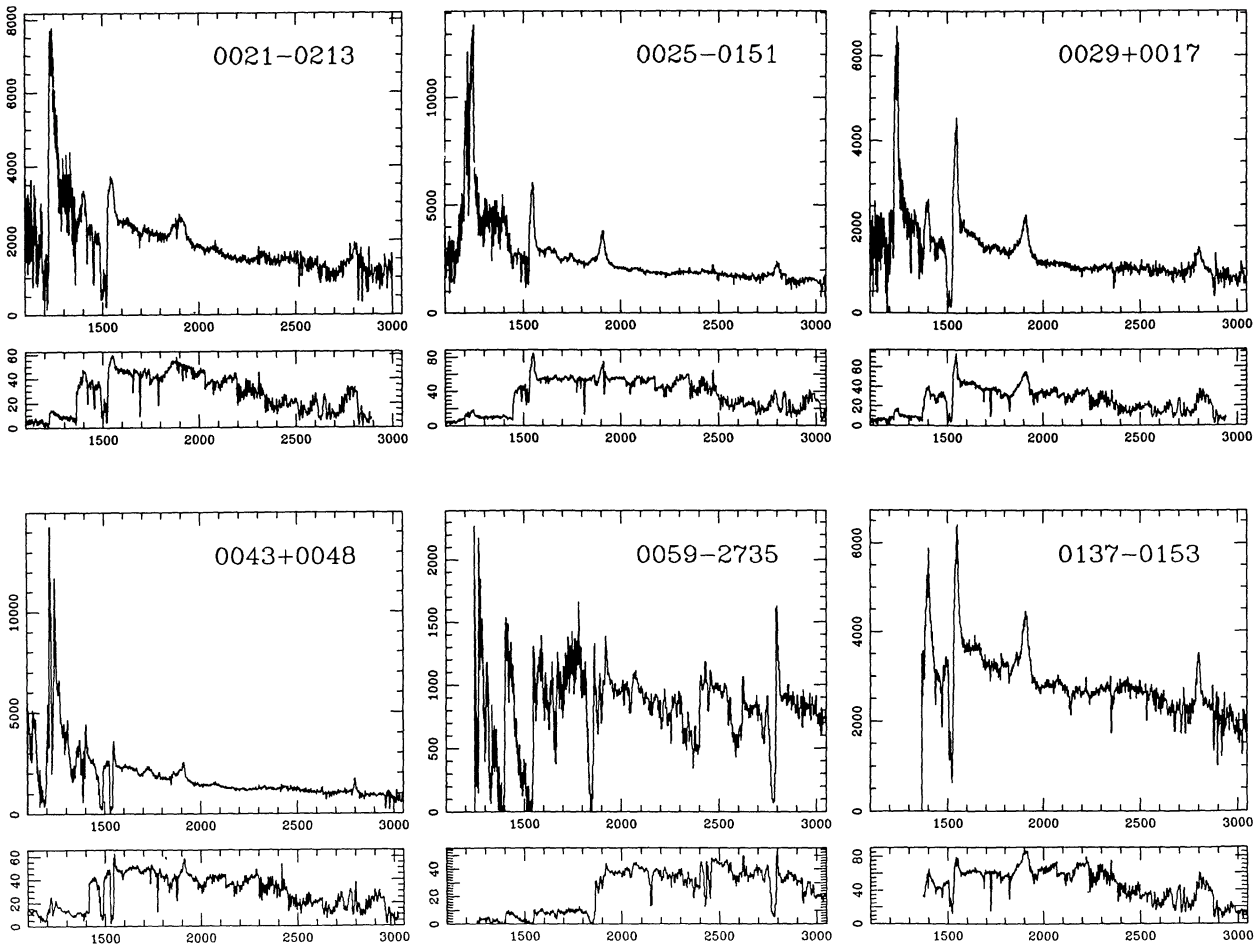

FIG. 1*b*

of the N v + Lyα blend redward from the N v peak to where the line appears to end. Other weak features (Si II, O I) make this uncertain, but setting the level of the continuum is almost always a larger source of uncertainty. The index, given in column (9), contains a small contribution from Lyα as well as N v, but, as emphasized above, we are interested in measuring differences between BALQSOs and non–BALQSOs even if the indices are not "pure."

3.2.2. *Emission-Line Strength of the Red Half of* C IV λ1549

The presence of the C IV absorption troughs in the BALQSOs makes it virtually impossible to compare the strengths of the entire C IV emission line in the non–BALQSOs to those in the BALQSOs. There is some hope of measuring only the red half of the C IV line. However, as discussed in § 4, there are frequently blueshifts of the C IV emission in both the BALQSO and the non–BALQSO objects with respect to the Mg II emission. If the Mg II peak is a more accurate estimate of the true rest system of the object, and there is significant absorption at velocities near zero in this rest system, then the strength of even the red half of the C IV could be affected.

We used the spectra which had been normalized by the rough continuum described above for the case of N v, and likewise rederived a local continuum underlying the red half of the C IV emission, estimated the wavelength of the peak of the C IV emission, and measured the equivalent width from that peak to where the observed flux intersected the local continuum.

The estimation of the local continuum, while not as uncertain as in the case of N v, is made difficult by the presence of the C IV absorption troughs in the BALQSOs and also by blending with other emission to the red, including He II λ1640. The mean spectra described in § 5 as well as the composite spectrum of Francis et al. (1991) give the strong impression of very broad C IV wings underlying the main core of the line, but the absorption troughs and the blending to the red make it impossible to measure the contribution from this component. Inspection of the spectra normalized by the rough continua showed that the region from about 1575 to 1625 Å was quite flat with often a shallow minimum around 1600 Å. We therefore set the local continuum to the value of the normalized flux at 1600 Å, or to the value at which the normalized flux passed through the shallow minimum if this point occurred shortward of 1600 Å. This procedure therefore measures the red half of the core of the line but omits much of the contribution from any underlying broad wings. This index, while still involving some subjectivity, is not nearly as uncertain as the N v. The values for this index are given in column (10) of Table 2.

3.2.3. *The* C III] λ1909 *and* Al III λ1857 *Strengths*

As noted in § 1, previous investigators have concluded that "Al III λ1857" was anomalously strong, and it has also been

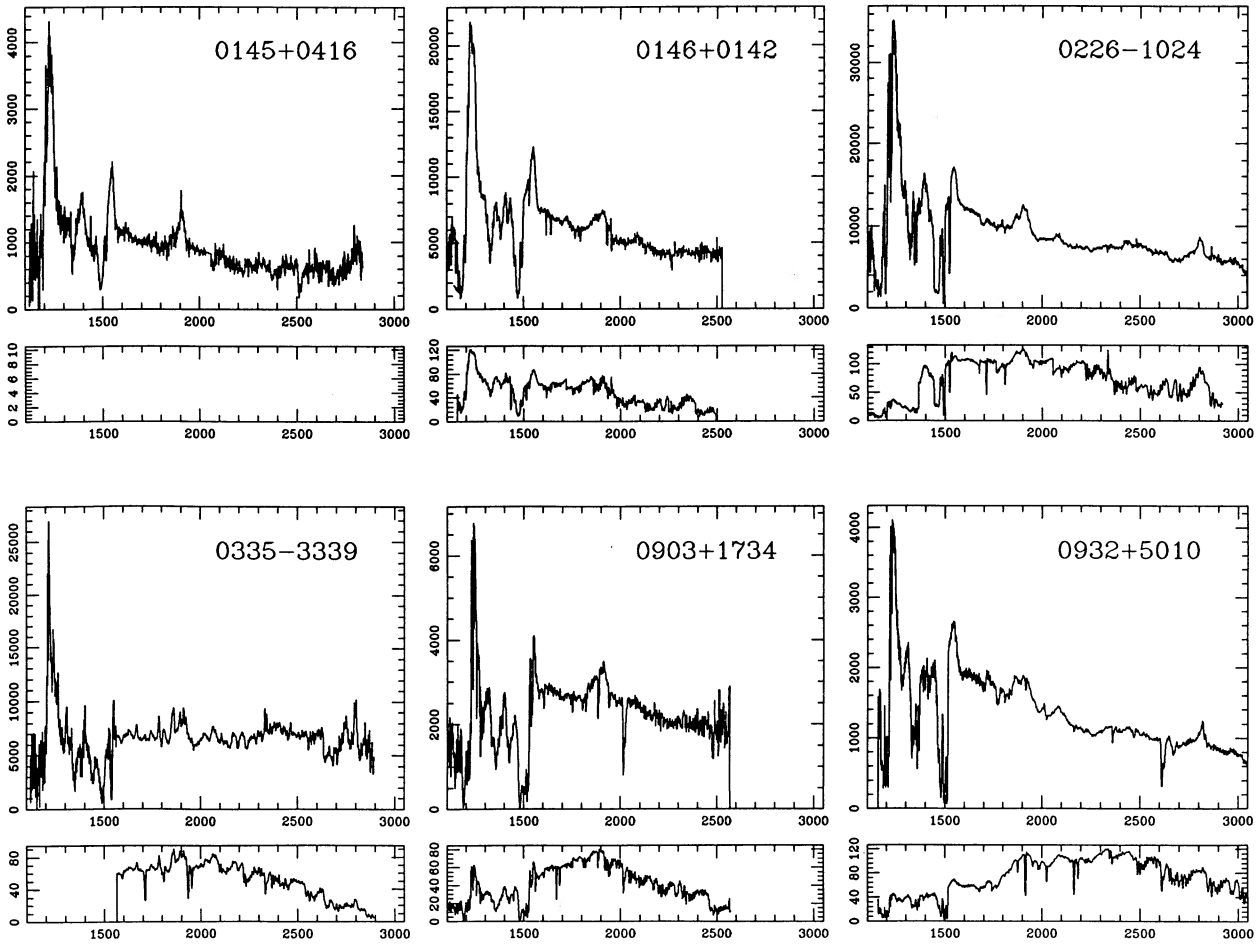

FIG. 1c

observed that "C III] λ1909" was anomalously wide in BALQSOs. The anomalous width of the "C III]" has generally been attributed to cases where blending due to the "Al III" was not taken into account. We have enclosed these two transitions in quotes because in at least one object, HB present strong evidence that the emission near 1909 Å is actually dominated by a blend of Fe III lines. The identification of the feature around 1857 Å with Al III is probably correct, but in many non–BALQSOs, as well in BALQSOs, it is very much stronger than can be understood on the basis of simple photoionization models with solar abundance ratios of Al/C (Uomoto 1984; Boyd & Ferland 1987). In § 5 we discuss additional evidence that there are other contributors besides Al III and C III] in this region of the spectrum.

We carried out the deblending of the C III] and Al III by using an algorithm very similar to the deblending algorithm subsequently implemented in IRAF, namely: (*a*) We defined by eye a local effective continuum, linear in wavelength, and passing through local flux minima at about 1800–1820 Å and 1975–2000 Å. (*b*) We used the Levenberg-Marquardt chi-square algorithm MRQMIN given by Press et al. (1986) to fit two Gaussian components. If all six of the parameters were initially regarded as free, we found that there was substantial sensitivity of the final values of the fitted parameters (or even the obtaining of convergence of the routine) to the input parameters. Therefore, we first fitted a single Gaussian in the vicinity of the C III] to locate the wavelength of the C III] component. (*c*) We then froze that wavelength and used MRQMIN to fit the remaining five free parameters. (*d*) We assessed the significance of the Al III component by comparing the fit to the noise spectrum. For eight of the objects (noted in Table 2) we regard the measures as being only upper limits to the Al III. However, in the subsequent statistical analysis they are treated as detections. In one or two of the objects Si III λ1892 may be just resolved from C III], but in general it is impossible to separate Si III from C III] in our sample. The equivalent widths of Al III and C III] and the ratio Al III/C III] are given in columns (11), (12), and (13) of Table 2.

3.2.4. *The* "Fe II λ2400 *Index*"

We define an index of Fe II strength which is very similar to, but not identical with, that adopted by Baldwin et al. (1989). In formulating it we were guided by inspection of the mean spectra formed from samples 1′ and 2′ (see §§ 4 and 5). We first attempted to use a wholly automatic algorithm, defined as follows: (*a*) Find the median values of the flux in each of the two windows 2240–2255 Å and 2665–2695 Å. (*b*) Define an effective continuum by assuming that the flux per unit wavelength is a linear function of wavelength, when fitted to the two median values at the midpoint of these windows. (*c*) Interpolate across any strong sharp absorption features, and, when the signature of the atmospheric A band is present, interpolate

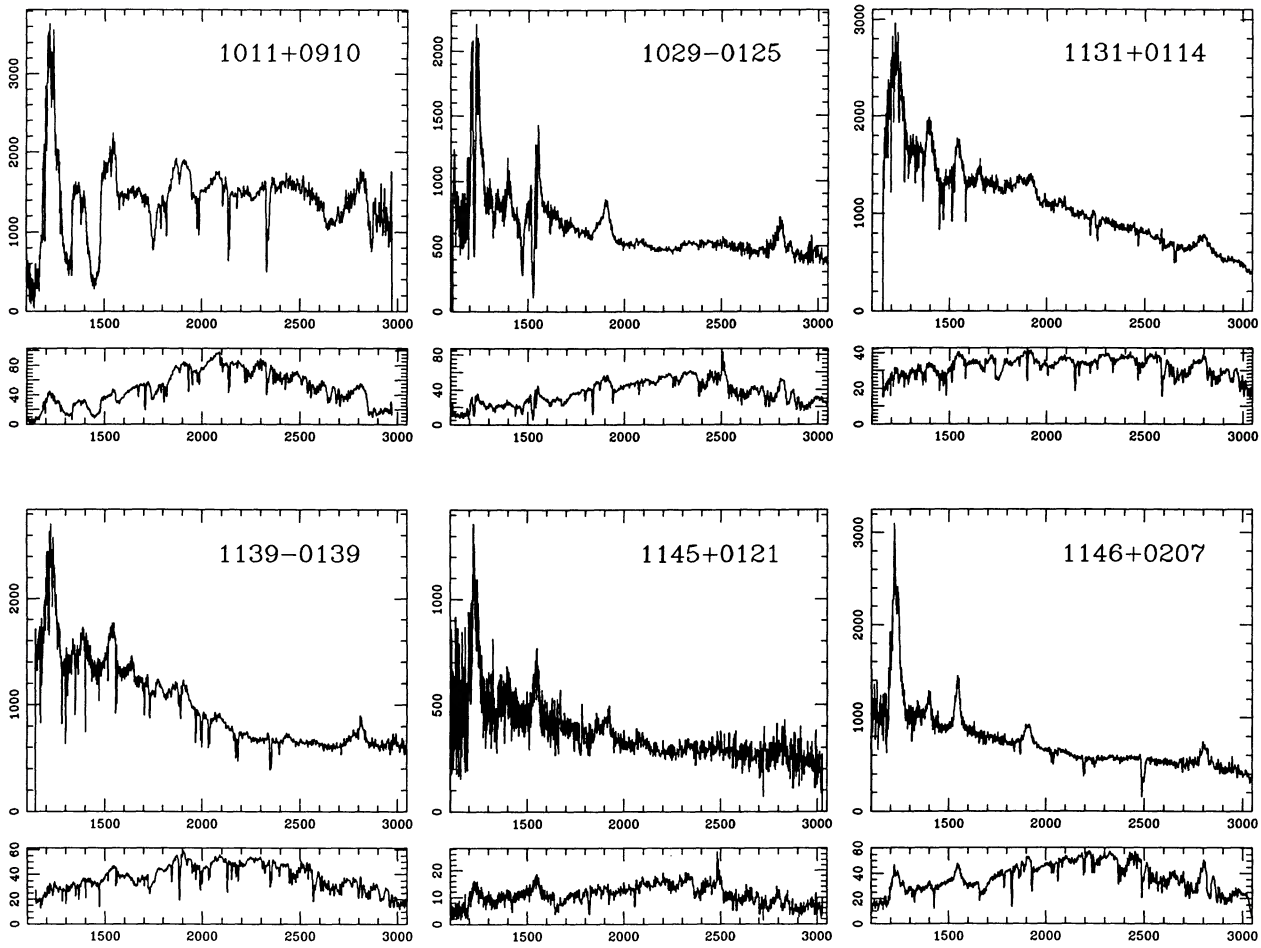

FIG. 1*d*

over that as well. (*d*) Find the equivalent width of the emission between 2255 and 2650 Å in terms of this effective continuum. As the composite spectrum by Francis et al. (1991) demonstrates, and as emphasized by Wills (1988), it is very likely that these windows are only local minima which still contain significant amounts of Fe II emission and are not true continuum windows. In the course of carrying out these measurements, it also became clear that the detailed shape of the Fe II emission varies from object to object, so that these points of minimum Fe II emission vary. A more serious difficulty is that for a few of the objects (notably 0059−2735) this automatic method of measuring the index fails because of obvious or incipient broad absorption associated with either Fe II or Mg II which falls within either the continuum-defining windows or the emission window. We proceeded by first locating the "continuum" using the automatic procedure just described and then making in a few cases adjustments (usually very small) to this continuum by eye. We always used the wavelength interval defined above for measuring the actual equivalent width.

While this situation is not very satisfactory, until reliable Fe II models for this part of the spectrum are available, we do not know how to improve on it. This Fe II index is given in column (14) of Table 2.

3.2.5. *The "2070 Å Index"*

Although the identification of this feature as Fe II is not certain, it is a well-marked feature in many QSOs and serves as a useful check on the measurement of the Fe II strength. In § 4 we confirm the result by HB that it is strongly correlated with the Fe II index, strengthening the case for this identification. We define it in exactly the same manner as the Fe II index, except that there are two continuum windows located at 1975–2000 Å and 2140–2155 Å. The flux is integrated between 2040 and 2130 Å. The same uncertainties and caveats for the Fe II index described above apply to this index as well, which is given in column (15) of Table 2.

3.3. *Line Widths*

We present only two measures of line widths: the half-width at half-maximum for the red half of C IV (with the caveats noted above concerning the effects of the absorption troughs on measurements of the C IV emission-line strength) and the half-width at half-maximum for the C III] line obtained as a result of the deblending from Al III described above. These two measurements are given as columns (7) and (8) of Table 2. It is obvious that there is a large difference between the two sets of widths in the sense that the C IV is considerably narrower.

This difference cannot necesarily be interpreted as a real difference in line width, and it must be recalled that the two sets of widths were obtained in two different ways: in the case of the C IV, we directly measured the half-width at half-intensity. In the case of the C III], the half-width at half-maximum is derived from a Gaussian fit to two components. Moreover, in this

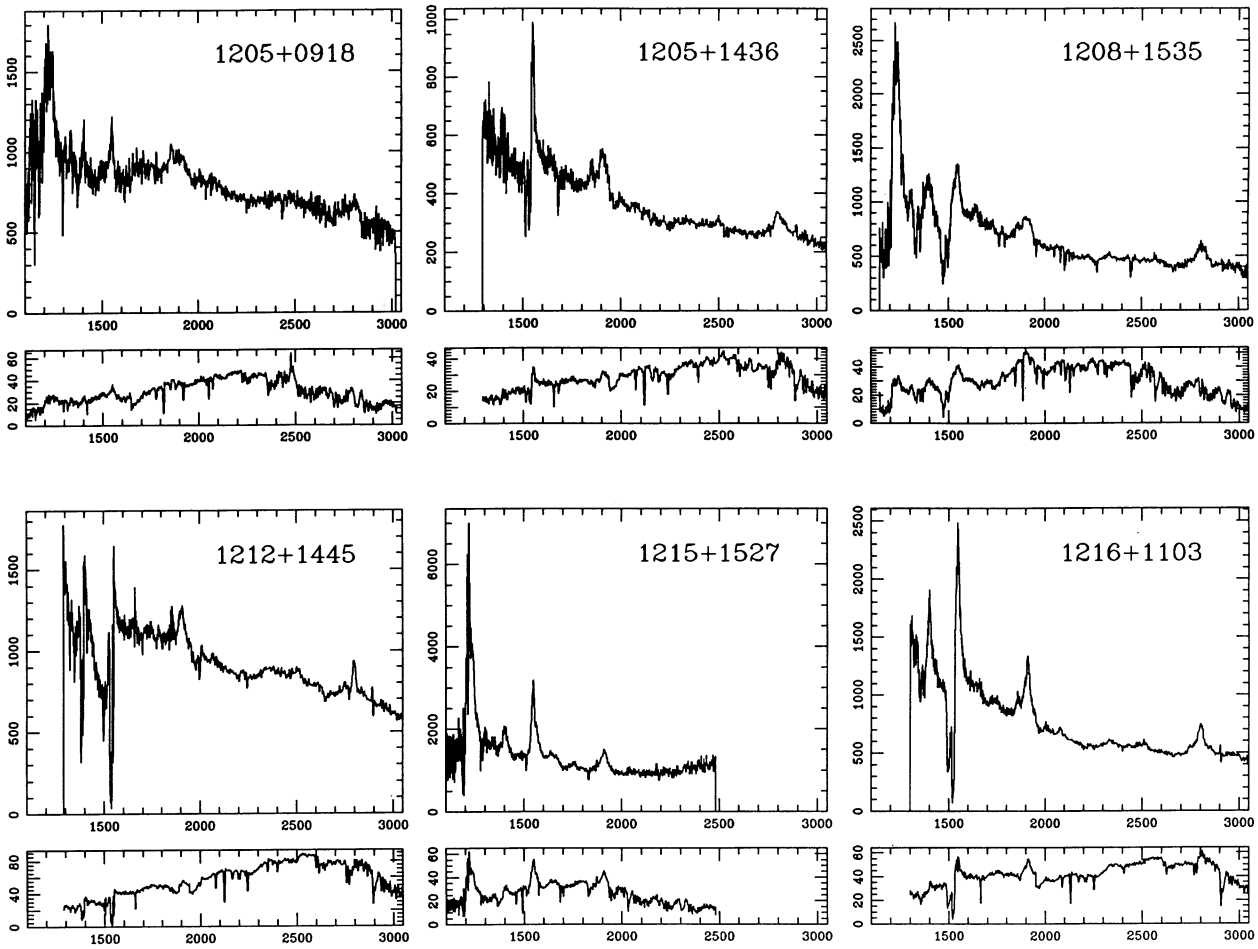

FIG. 1*e*

region of the spectrum there are almost certainly other important contributors which are blended with the C III] and increase its apparent width even after it has been deblended from the Al III.

We have not attempted to measure either the strength or the width of Mg II for individual objects, although we attempted to measure the peak wavelength. In too many cases the redshifts of the objects are sufficiently high that the Mg II line does not have adequate signal-to-noise ratio or is not observed at all. In § 5 we describe the properties of the Mg II line on the basis of the mean spectra.

The remaining columns in Table 2 are explained in § 4.

4. DEFINITION OF SAMPLES AND RESULTS OF STATISTICAL TESTS

4.1. *Definition of Some Statistical Samples*

Before carrying out the statistical tests, we define several subsamples on which these tests will be performed:

Samples 1 and 1′.—The non–BALQSO samples. Sample 1 is composed of all the objects in Table 2 with zero value of the balnicity index. Sample 1′ is identical to sample 1, except that we have treated the two marginal BALQSOs in the middle section of Table 2 as non–BALQSOs. Note that the non–BALQSO samples consist only of objects found in the LBQS.

Samples 2 and 2′.—The BALQSO samples. Sample 2 is composed of all the objects in Table 2 with nonzero values of the balnicity index, including the two marginal objects. Sample 2′ excludes these two marginal objects.

4.1.1. *Some Further BALQSO Subsamples*

It is appropriate to define further subsamples among the BALQSOs. In order to avoid the number of different combinations of objects to be tested from unreasonable proliferation, we will consider, for the purposes of defining these BALQSO subsamples, that the two marginal BALQSO objects are *not* BALQSOs: i.e., we will consider sample 2′ to be the BALQSO sample from which various BALQSO subsamples are drawn. The results below suggest that this choice acts to accentuate mildly the differences between the BALQSO and non–BALQSO samples.

As noted in § 2, our BALQSO sample is a mixture of objects which were found in the LBQS survey and BALQSO found by other means. (Some LBQS objects are in fact also well-known BALQSOs, as is evident from inspection of col. [10] in Table 1). Some bias may be introduced because of this. We therefore define

Sample 3.—All BALQSOs found in the LBQS.
Sample 4.—All BALQSOs not found in the LBQS.

In column (2) of Table 2 we list the samples to which each object belongs. Six additional subsamples (5–10) are defined and discussed below. We will make frequent references to

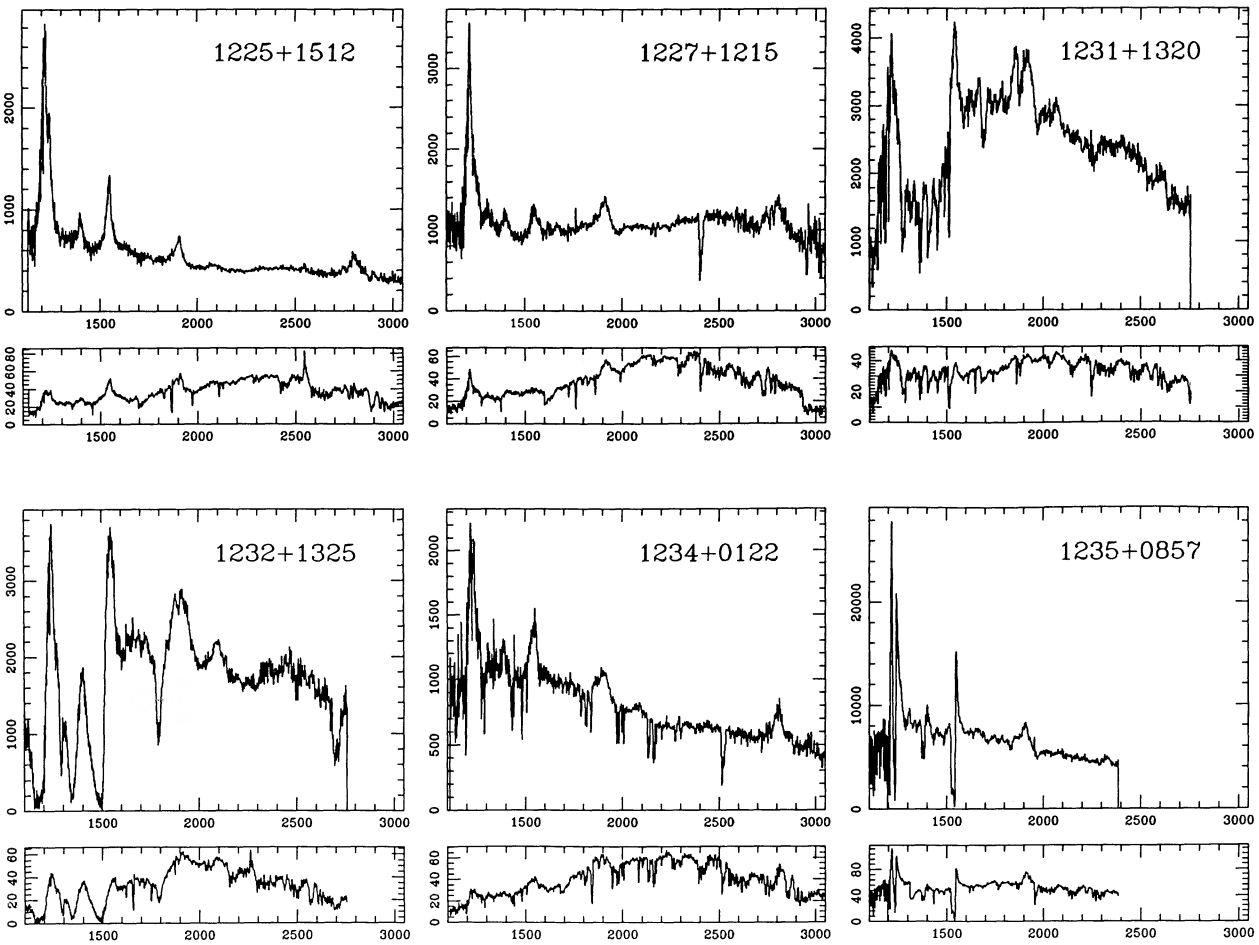

FIG. 1*f*

various samples and subsamples throughout the remainder of the discussion. As an aid to the reader, we give in Table 3 a concise summary of the definitions of the various samples.

4.2. *Results of Statistical Analysis*

The medians, means, and rms values for the emission-line indices and line widths for the entire sample and each of the statistical samples are contained in Table 4, which also contains the number of objects in each sample. Note, however, that not every index has been measured for each object in a particular sample.

Each element in the sample-index matrix consists of three entries. The first is the median, the second is the mean, and the third is the accompanying rms value.

4.2.1. *Analysis of the Pure LBQS Samples*

Let us first confine our attention to a comparison of sample 1′ and sample 3, that is, between the non–BALQSOs and the BALQSOs, all of which are selected from the LBQS, thereby minimizing differences attributable to any selection effects. Inspection of Table 4 indicates that regardless of the statistical significance which may or may not be ultimately established between differences in the emission-line properties of the non–BALQSOs and the BALQSOs, these differences are *subtle*. In fact, if we form measures of the differences in the means of the indices of the form

$$\frac{2|(\text{sample } 1' - \text{sample } 3)|}{(\text{sample } 1' + \text{sample } 3)},$$

then among the seven line-strength indices and the C IV and C III] line-width indices for these two samples we find that the largest difference (for the N V index) is only 22%.

To see whether any of these small differences are in fact statistically significant, we use the Kolmogorov-Smirnov test as implemented in the IRAF–STSDAS statistics package KOLMOV. The results of these tests are summarized in Table 5.

Across the top of Table 5 we list the pairs of samples against which the K-S test is run for each of the indices listed in column (1). Each entry in the element of the sample pair–index matrix gives the percentage of times that the measured K-S statistic would be exceeded by chance. Since one of the line-strength indices (e.g., the ratio of Al III to C III]) cannot be considered statistically independent of the Al III and C III] indices, there is a total of (2) line-width and (6) line-strength indices which are really independent. Thus, we might expect about one value of order 10% to occur by chance. Inspection of the entries for the sample pair (1′, 3) shows that among the line-width and line-strength indices the most significant result is for the N V strength index, but only at a level of 7%. This

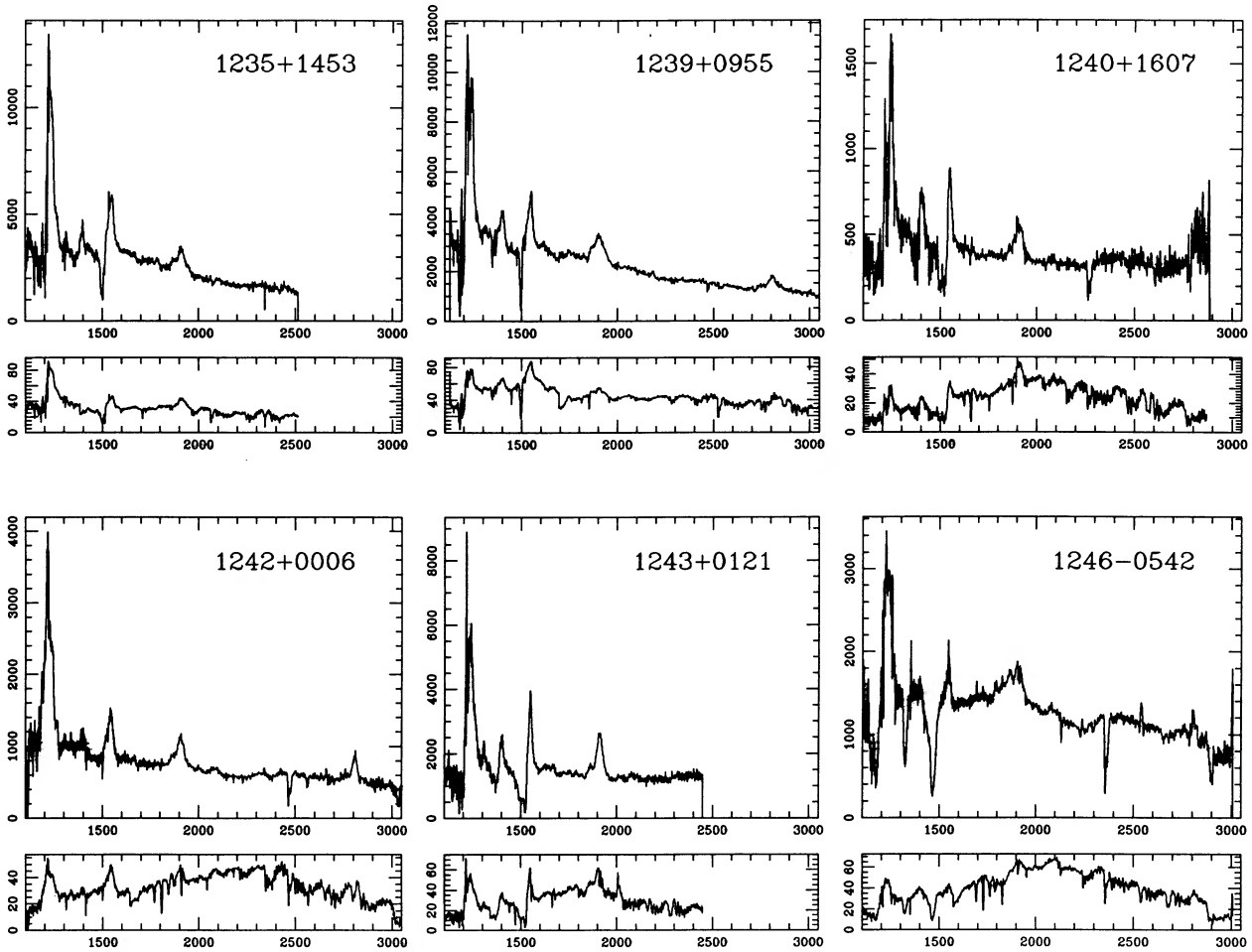

FIG. 1*g*

bears out the results of Table 4 that among the LBQS non–BALQSO and BALQSO samples the emission-line properties differ only very subtly.

4.2.2. *Analysis of the Full Set of BALQSOs*

When we compare the full set of BALQSOs with the non–BALQSOs, the situation changes. We have considered two possible ways for carrying out this comparison: we can compare the entire set of BALQSOs, both the ones found in the LBQS survey and the previously known ones (sample 2′) with the non–BALQSOs (sample 1′), or we can compare only the BALQSOs *not* found as part of the LBQS (sample 4) with sample 1′.

Considering the former possibility first, inspection of Table 5 shows that two of the differences in the indices and their statistical significance are substantially increased: the evidence for stronger N v in the BALQSOs is now more compelling (at 2%), and in addition there is some evidence for a difference between the Al III index at the 3% level in these two samples. In the case of these two indices, the statistical significance is somewhat higher when the two marginal BALQSOs described in § 3 are considered part of the non–BALQSO sample [sample pairs (1′, 2′)] as opposed to being considered bona fide BALQSOs [sample pairs (1, 2)]. This is the reason for our remark above that considering the two marginal objects as non–BALQSOs accentuates any differences that might be present.

Alternatively, if we compare only the BALQSOs *not* found in the LBQS (sample 4) with sample 1′, then Table 5 indicates that the significance of the N v index difference is actually weaker than for the LBQS BALQSOs, but the significance of the Al III difference is much stronger—0.2%. There is also a suggestion of a difference in the Fe II λ2400 index at 5.4%. We interpret this to mean that there was nothing atypical about the known BALQSOs as far as N v is concerned—a small real difference between the N v strength of BALQSOs and non–BALQSOs may simply become more statistically significant as the sample size is increased. However, there may be differences in the Al III and possibly Fe II properties between the known BALQSOs and those found in the LBQS, for reasons not understood.

In general, we consider the K-S tests to be convincing in and of themselves only for probabilities of 1% or less, and merely suggestive for probabilities in the range from 1% to 5%. Taken together with supporting evidence from a quite different method of analysis, however (see § 5), these results in the 1%–5% regime can become fairly convincing.

4.2.3. *Definition of Additional BALQSO Subsamples*

The fact that the sample of known BALQSOs may differ from the LBQS BALQSOs lead us to consider whether there

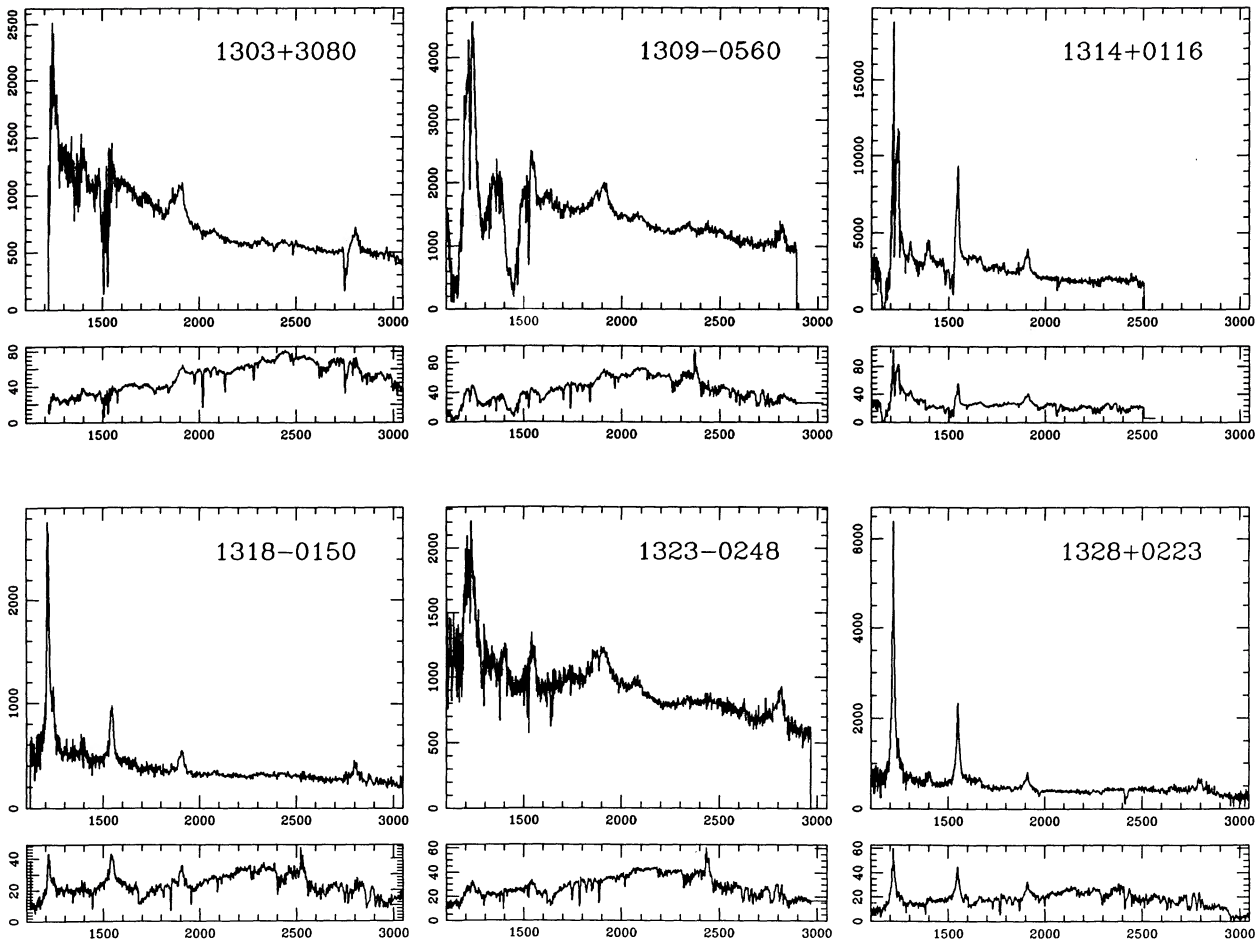

FIG. 1*h*

might be properties of the BALQSOs which biased the sample of known BALQSOs and which are correlated with emission-line properties. More generally, we would like to know whether there are correlations between specific properties of the BAL troughs which correlate with emission-line properties regardless of the method of sample selection. An obvious case in point is the object 0335−3339 (Hazard et al. 1984; see also HB), which was picked out as being interesting because of its very strong and sharp Fe II emission.

In formulating various subsamples to explore these questions, it must be admitted that we are groping for clues without benefit of secure physical models to guide us. However, one obvious measure of the property of the BAL troughs which might be correlated with emission-line properties is the balnicity index itself. The balnicity index might also enter as a selection effect in the known BALQSO sample, since objects with the strongest troughs are most likely to be noted as BALQSO candidates by visual inspection of objective-prism plates. We therefore divided all the BALQSOs into two groups, those having balnicity index above and below the median value. This leads to

Sample 5.—BALQSOs with large balnicity index.
Sample 6.—BALQSOs with small balnicity index.

It was noted by HB that there appeared to be a subclass of BALQSOs, namely, those with "detached" troughs, which showed the largest emission-line differences from the non–BALQSOs. In Appendix B we consider various ways to define a "detachment index." Experiments with the correlation between the emission indices and various definitions of this index demonstrated that some mild correlation appeared to exist when we utilized the detachment index associated with the strongest trough (see the discussion in Appendix B.) It is this detachment index which we use in column (4) of Table 2. In order to apply the K-S test to see whether BALQSOs with large detachment indices differ significantly from non–BALQSOs in their emission-line properties, we divided the sample 2′ BALQSOs into two groups above and below the median of this detachment index. This leads to

Sample 7.—All BALQSOs with large detachment indices.
Sample 8.—All BALQSOs with small detachment indices.

As discussed in § 5, the relatively small number of BALQSOs in our sample which have low-ionization absorption troughs (Al III and Mg II) appear to have properties which distinguish them from the rest of the BALQSOs. The selection of objects and the assignment of associated weights which define BALQSOs with and without low-ionization troughs is described in § 5 and leads to

Sample 9.—All BALQSOs with evident low-ionization troughs.

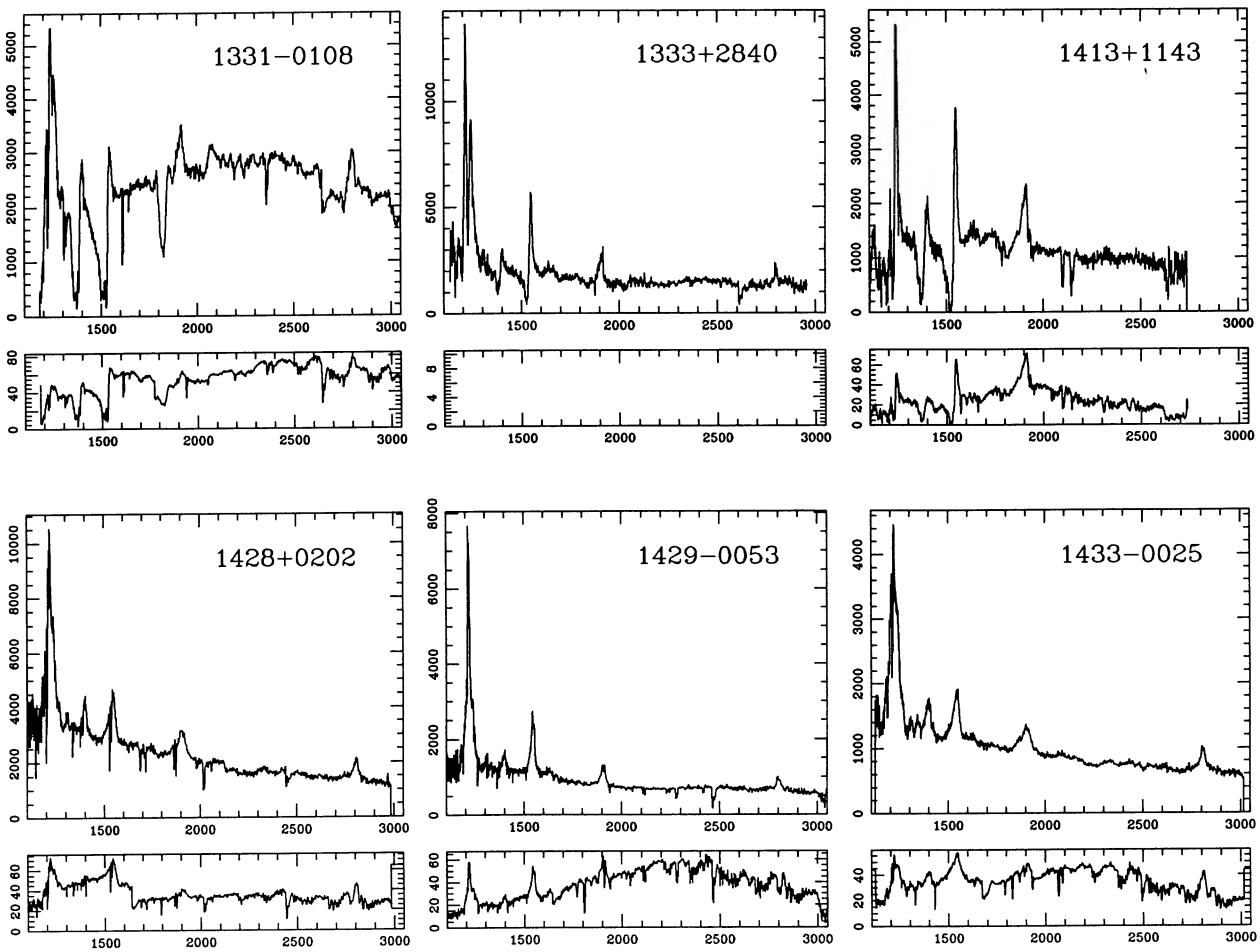

FIG. 1*i*

Sample 10.—All BALQSOs with very weak or no low-ionization troughs.

Note that those objects which have weights less than 1.0 and greater than 0.0 appear in both samples 9 and 10.

4.2.4. *Analysis of the Additional BALQSO Subsamples*

We first examine whether there are any significant correlations involving the properties of the BAL troughs as measured by the balnicity and detachment indices. We used the Press et al. (1986) algorithms to carry out three nonparametric tests using the parameters Spearman *d*, Spearman *rs*, and Kendall τ. In Table 6 we present the result of running these correlation tests.

The first two columns list the two indices for which the correlation is being tested, and column (3) gives the number of objects involved in the test. Column (4) gives the probabilities (*in percentages*) that the correlation statistics given by the correlation tests just enumerated would occur by chance at a level greater than the measured value. In general, the three tests give quite consistent results, and we have listed only the probability associated with the Kendall τ test, except for the cases where a significant correlation is indicated ($P \leq 2\%$), where we also give the results for the two Spearman tests.

Inspection of the entries in Table 6 shows that there are some correlations which are significant. In particular, we consider first those associated with the Fe II $\lambda\lambda$ 2070 and 2400 indices versus the balnicity index, both of which are highly significant.

Note from Table 4 that the Mg II BALQSOs (sample 9) have significantly higher than average balnicity indices and Fe II indices. It might therefore be thought that the balnicity index–Fe II correlation arises solely from the objects in sample 9. However, Table 6 shows that even when these objects are removed, the evidence for a balnicity index–Fe II correlation remains strong. As mentioned in § 3, the strong λ2400–λ2070 correlation noted by HB strengthens the case for the λ2070 feature as being due to Fe II.

In Figure 2 we plot the λ2400 index against the balnicity index for all the objects in sample 2′.

Table 6 also provides some evidence for an anticorrelation of the detachment index with both the C IV and C III] strengths. The former cannot be due to the fact that the least detached troughs eat into the C IV emission more than do the highly detached troughs, since the effect is in the wrong sense: the least detached troughs are the ones whose strengths would be most affected by the absorption, yet they are the strongest. These correlations could arise because the detachment index (Appendix B) involves division by a measure of the emission-line width, and if the line strengths and line widths were correlated, this in turn could account for the correlation of line strength with detachment index. However, we find no evidence for a line-width–line-strength correlation.

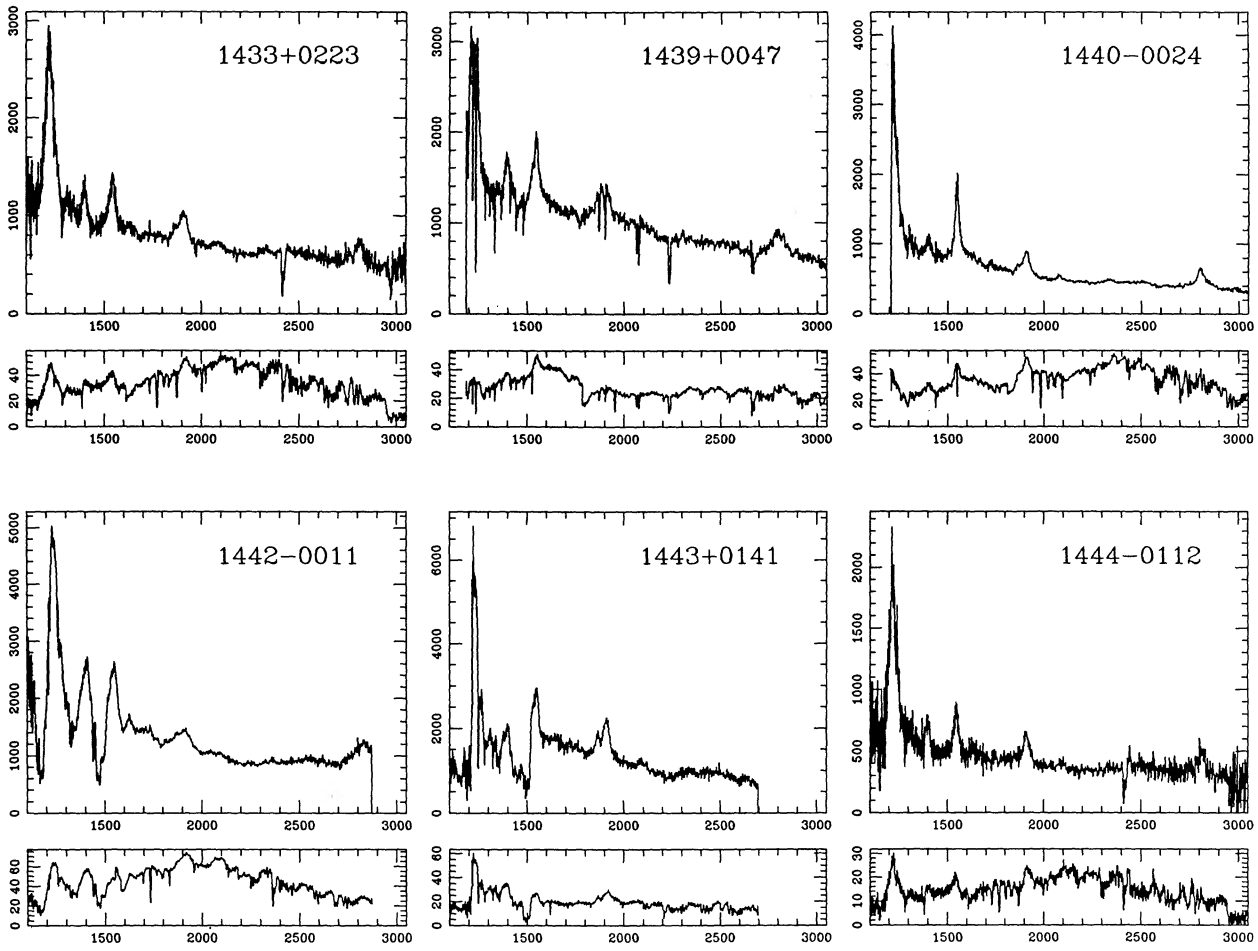

FIG. 1*j*

Our result is consistent with the tendency for the absorption systems with smooth "PHL 5200–like" troughs (which are generally not detached) to have larger C IV emission peak/continuum ratios than the systems with complex troughs, an effect first pointed out by Turnshek (1984b).

In addition to the correlation tests, we can also run K-S tests on the subsamples (5–10) defined above against sample 1′. Because of the weights assigned to objects in the low-ionization BALQSO sample (§ 5), it is not possible to use the correlation or K-S tests with the weighted samples 9 and 10 in a straightforward way. In the case of samples 9 and 10, therefore, *for the purposes of the K-S tests, correlation tests, and the data in Table 4*, we assigned weights of 1.0 to all the objects in sample 9 which actually had weights greater than 0.5, and weights of 0.0 to those actually having weights less than 0.5.

None of the K-S tests involving samples 5–10 have probabilities less than or equal to 1%, and, as remarked above, the several which have $1\% \leq P \leq 5\%$ should be considered suggestive rather than conclusive, but nevertheless warrant comment: since sample 10 differs only slightly from sample 2′, the N V result for sample 10 is not surprising. However the N V results for samples 5 and 8 are mildly surprising in that no evidence for a correlation between the N V strength and balnicity index or detachment index was found. Since the K-S test can measure differences in the distribution between two samples even though the means of the two samples are about the same, it may be that the mild evidence for significance in these two samples arises from the dispersion in the N V index for the BALQSOs, which in turn is partly due to the difficulty in defining the continuum.

The Fe II $\lambda\lambda$2070 and 2400 results for sample 5 are not unexpected given the Fe II–balnicity index correlation. The 1.6% result for Al III for sample 8 is a bit unexpected given the absence of any evidence for enhancement of Fe II in sample 8, and given the evidence for an Fe II–Al III correlation. Although the entries for both Al III and C III] for sample 5 are both below 5%, there is no evidence for enhancement of the *ratio* of Al III to C III] (as reported by HB). Our result can perhaps be understood if it is true then whenever the "Al III" emission is enhanced in the sample the C III] is also enhanced, but by a slightly smaller amount. As discussed in § 5, the interpretation of these results in terms of enhanced Al III and C III], especially for samples involving the Mg II BALQSOs, is suspect.

4.3. *Velocity Shifts*

One expects no differences in emission-line indices between BALQSOs and non–BALQSOs if there are no *intrinsic* differences between the two sets of objects *and* if the emission is isotropic. The same is not necessarily true for velocity shifts between emission lines of different species. If the velocity fields

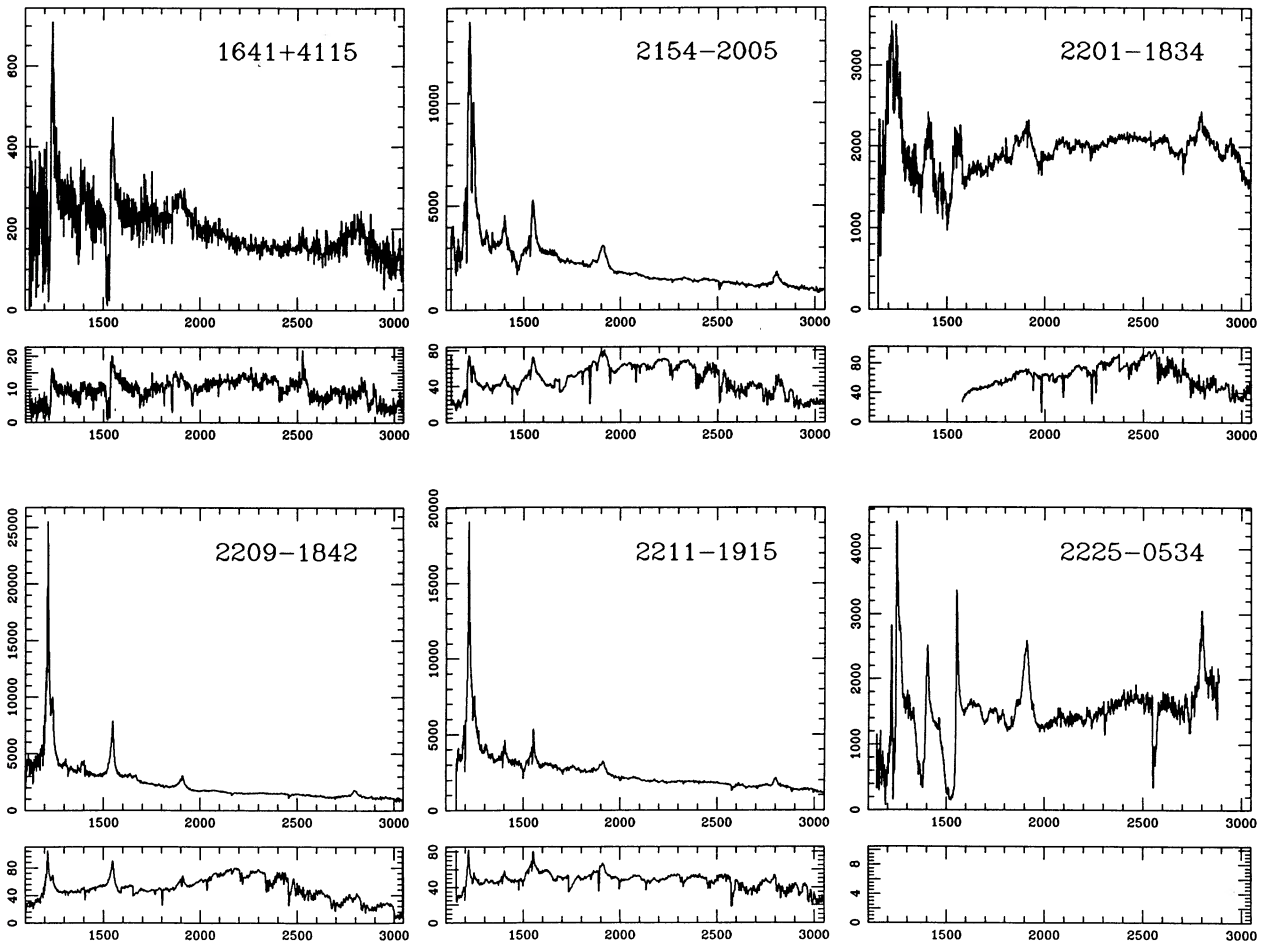

FIG. 1*k*

associated with any of the lines are not isotropic (or if there is significant obscuration of portions of the emitting regions), then systematic differences in viewing angle between BALQSOs and non–BALQSOs might result in differences in these velocity shifts. Recent work by Corbin (1990a), as well as previous work by Gaskell (1982), Wilkes & Carswell (1982), and Espey et al. (1989), has shown that systematic velocity shifts between the emission lines of different ions are common. (However, this result appears to depend somewhat on how the sample of objects has been selected, since other samples show only very small or no shifts (cf. Junkkarinen 1989). In particular, Corbin (1990b) reports that velocity shifts correlate with luminosity, and that, for a given luminosity, the BALQSOs have larger shifts than the non–BALQSOs (Corbin 1990a, b).

We have attempted to measure the peaks of the C IV, C III], and Mg II lines in as many objects of our data set as possible. The C III] peak wavelengths were taken from the C III]–Al III deblending procedure described in § 3. The C IV and Mg II peaks were measured by eye, and these measures compared with the results of an automated algorithm which found the midpoints of the lines at various fractions of the peak height. There was generally good agreement between the eye estimates and the computer algorithm when the fraction was set at 65% of the peak intensity. Exceptions to this agreement occurred for very noisy profiles (where the eye estimate corresponded to midpoints of 40% or 50% of the peak intensity), profiles badly cut up by sharp absorption, and strongly asymmetric profiles (in which case the eye estimates correspond to midpoints much closer to the peak intensity). The values presented are in fact based upon the eye estimates, since these probably correspond most closely to what previous observers have measured. In any case, there are only a small number of cases where the disagreements between the eye estimates and the computer algorithm are in excess of 200 km s^{-1}.

The velocity shifts between C IV and C III] and between C IV and Mg II are presented as columns (5) and (6) of Table 2. A positive velocity means that the C IV peak is shifted to the blue of its expected position relative to C III] or Mg II. The correlation tests previously described applied to the C IV–C III] and C IV–Mg II shifts yield a high level of significance as shown in the last line of Table 6, confirming one of Corbin's results. Significant velocity differences between these two pairs of lines could result from a shift of just one of the three line peaks. The correlation we have found would require that this line be C IV. However, the fact that the C IV-C III] shifts are much smaller than the C IV–Mg II shifts makes this implausible. We conclude that both C IV and C III] are shifted with respect to Mg II, whose shift, based upon previous work, is probably quite small compared with the rest system defined by the narrow emission lines. A formal regression analysis for the C IV–C III] and

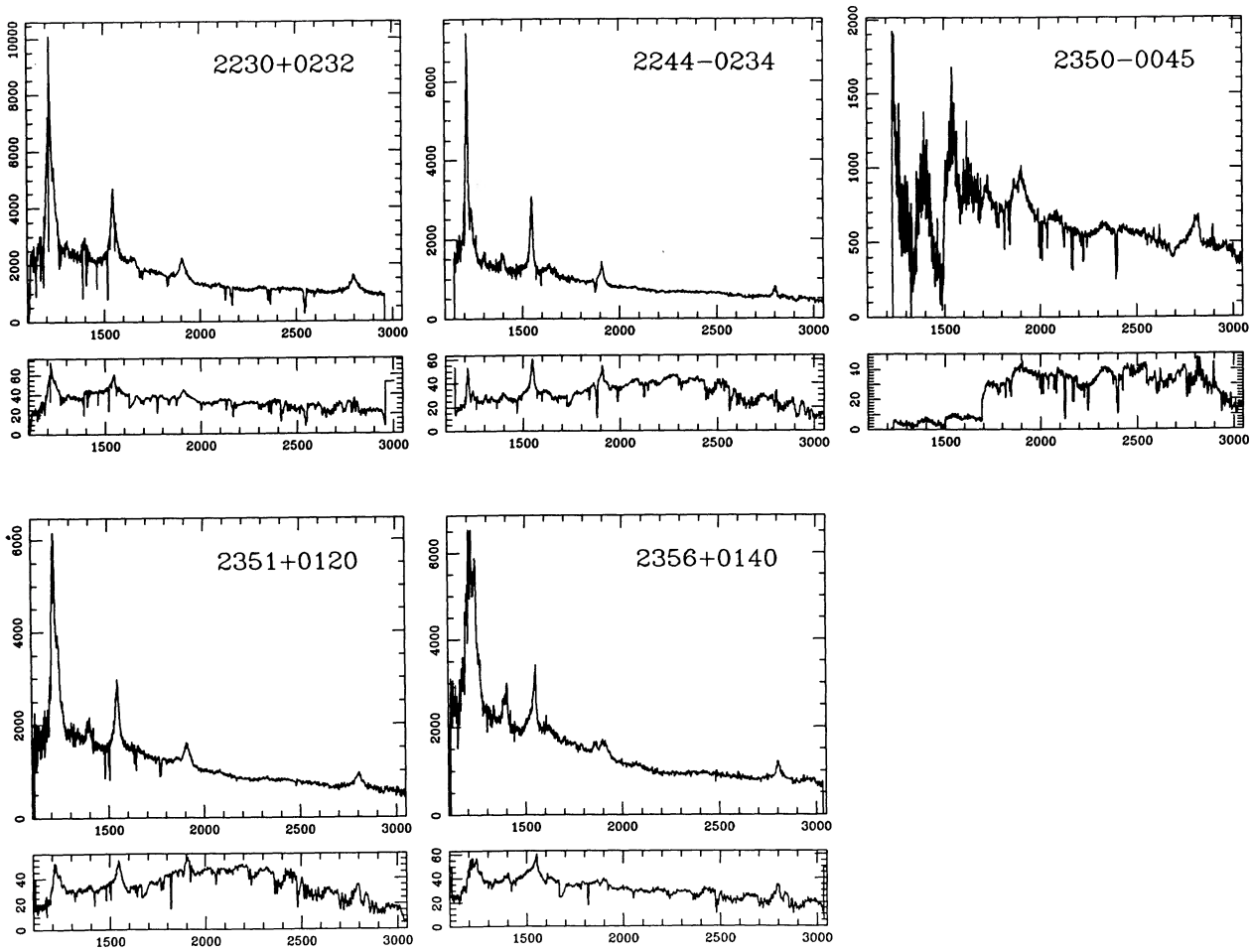

FIG. 1*l*

C IV–Mg II shifts gives

$$V(\text{C IV} - \text{Mg II}) \approx (1000 \pm 100) + (0.65 \pm 0.11)(\text{C IV} - \text{C III}]) \text{ km s}^{-1} .$$

The medians, means, and rms values for the velocity shifts are given in the top two rows of Table 4. Since the shift of C IV with respect to Mg II is much larger than that with respect to C III], we will confine attention to the C IV–Mg II shift. Examination of the entries for samples 1′ and 2′ in Table 4 suggests that the BALQSOs do not have larger shifts than the non–BALQSOs; if anything, the shifts appear to be slightly smaller in the BALQSOs than in the non–BALQSOs. This is in disagreement with Corbin's result.

The K-S tests for the distribution of velocity shifts given in the first two rows of Table 5 show no value below 5% except for sample 8, the sample with small detachment index. We found that the BALQSOs with small detachment indices did not have weaker than normal C IV emission, as might have occurred if the red half of the emission were systematically being strongly eaten into by the absorption troughs—in fact, the emission seemed to be strongest in those objects. By contrast, however, it appears that our estimates for the C IV peak velocity may have been affected as demonstrated by the difference for the velocity shifts between the objects with large and small detachment indices in samples 7 and 8. One might suppose that such an effect could mask a real C IV–Mg II shift in the BALQSOs which is larger than that in the non–BALQSOs. However, this seems not to be the case, since the mean shift for the BALQSOs with large detachment indices, whose emission peaks are least likely to be affected by the absorption troughs, agree very well with the non–BALQSOs.

The results of the correlation tests for luminosity-velocity shifts are given in the next-to-last two rows of Table 6 and show no compelling evidence for such a correlation. However, our luminosity baseline is so small that it is not an adequate test. Note also, though, that our failure to confirm Corbin's result, that greater velocity shifts occur among the BALQSOs than among the non–BALQSOs, cannot be ascribed to luminosity differences between our BALQSO and non–BALQSO samples. Not only are the differences very small; they are also in the wrong sense to account for our null result if Corbin's result, that velocity shifts increase with luminosity, is correct.

5. CONTINUUM PROPERTIES, MEAN SPECTRA, AND Mg II BALQSOs

5.1. *Continuum Properties and Mean Spectra of the Non–BALQSOs and BALQSOs*

Rather than compare fitted continua with the individual spectra, we investigate whether there are significant differences

TABLE 2

MEASURED INDICES FOR INDIVIDUAL OBJECTS

Object	Samples	BI	DI	V (CIII]-CIV)	V (MgII-CIV)	CIV HWHM	CIII] HWHM	NV HREW	CIV HREW	AlIII REW	CIII] REW	AlIII/CIII]	2400 REW	2070 REW	Notes
0006+0230	1,1′	0	–	877	1285	2864	4350	19.8	12.3	1.8	25.	0.07	54.03	9.68	b
0009−0138	1,1′	0	–	136	1150	2128	4115	25.7	8.4	4.4	23.4	0.19	36.92	3.19	
0009−0215	1,1′	0	–	-194	1190	3173	3502	17.	8.7	4.8	20.6	0.23	27.93	3.92	
0010−0012	1,1′	0	–	1153	2186	3309	3675	16.4	7.2	5.6	19.6	0.29	48.57	5.84	
0013−0029	1,1′	0	–	253	771	1838	3243	13.2	16.7	2.7	21.3	0.13	22.32	3.94	b
1131+0114	1,1′	0	–	2268	1690	3657	4421	17.6	6.5	5.4	11.2	0.48	11.42	5.06	
1139−0139	1,1′	0	–	3615	3578	4180	–	17.2	6.5	–	–	–	6.22	4.2	
1145+0121	1,1′	0	–	1336	–	2806	3212	15.9	9.4	7.1	16.	0.44	34.44	7.38	
1146+0207	1,1′	0	–	299	952	2535	3557	17.1	8.9	2.4	17.3	0.14	18.98	5.54	
1205+0918	1,1′	0	–	-1124	758	1335	5630	8.8	3.8	3.4	13.9	0.24	26.61	3.08	
1215+1527	1,1′	0	–	582	–	1722	3769	16.7	20.4	2.7	24.9	0.11	–	2.36	b
1225+1512	1,1′	0	–	-284	583	2128	2929	23.2	14.5	4.3	21.4	0.2	26.74	5.38	
1227+1215	1,1′	0	–	752	–	5457	4460	23.1	8.7	3.7	23.8	0.16	42.14	2.16	
1242+0006	1,1′	0	–	465	1776	2554	3361	22.7	12.4	7.2	30.6	0.24	39.91	4.68	
1318−0150	1,1′	0	–	679	1124	2167	1688	20.4	14.7	2.2	18.9	0.12	35.11	4.64	
1323−0248	1,1′	0	–	552	1884	2922	5740	12.2	6.5	5.9	23.1	0.26	34.58	4.33	
1328+0223	1,1′	0	–	-180	-301	1606	667	18.2	21.1	3.4	25.9	0.13	48.75	1.08	b
1428+0202	1,1′	0	–	368	1495	2961	3377	19.2	9.4	6.5	22.	0.3	28.09	7.84	
1429−0053	1,1′	0	–	399	903	1857	1680	17.2	15.3	1.9	21.1	0.09	30.08	1.36	b
1433−0025	1,1′	0	–	-76	1700	2748	3793	21.3	7.2	4.1	21.6	0.19	30.44	7.53	
1433+0223	1,1′	0	–	974	2413	3444	3691	17.2	8.8	4.2	19.8	0.21	34.08	5.76	
1439+0047	1,1′	0	–	–	758	2922	–	21.1	8.7	–	–	–	19.29	5.22	
1440−0024	1,1′	0	–	259	1096	2593	3125	22.7	14.6	4.5	25.1	0.18	17.49	5.66	
1444−0112	1,1′	0	–	905	2440	2554	2890	20.5	14.2	5.9	24.1	0.24	44.18	3.46	b
2209−1842	1,1′	0	–	-7	100	1296	3856	15.4	14.0	0.7	21.2	0.03	29.51	5.1	
2230+0232	1,1′	0	–	56	590	2574	3196	19.1	13.8	2.	20.5	0.1	19.84	2.02	
2244−0234	1,1′	0	–	282	460	1528	–	12.9	14.7	–	–	–	19.34	3.21	
2351+0120	1,1′	0	–	571	1101	2438	3212	17.1	12.2	3.	17.9	0.17	29.56	1.8	
2356+0140	1,1′	0	–	-1060	81	1180	3926	19.3	4.2	4.	14.6	0.27	21.14	1.9	
1234+0122	1′,2	4	10.06	-557	1087	2070	4672	7.5	4.6	3.2	18.9	0.17	21.75	5.3	
2211−1915	1′,2	27	0.31	136	373	1722	3377	18.9	7.3	3.	13.9	0.22	22.88	2.6	
0019+0107	2,2′,3,6,7,10	2409	4.65	-763	303	1432	4193	15.5	7.5	2.8	18.1	0.15	21.99	5.96	
0021−0213	2,2′,3,5,8,10	5752	3.14	463	–	3077	3856	36.2	7.7	4.7	17.2	0.27	46.74	3.56	
0025−0151	2,2′,3,6,8,10	2320	2.97	-59	212	1645	2528	25.5	10.9	4.7	23.4	0.2	19.9	1.96	
0029+0017	2,2′,3,5,8,10	5693	2.45	-1	765	1857	3219	16.4	15.1	6.6	31.7	0.21	27.34	4.99	
0043+0048	2,2′,4,5,7,10	5082	10.06	344	227	987	1586	22.9	2.8	5.6	12.5	0.45	44.66	4.8	b
0059−2735	2,2′,3,5,8,9	11259	1.18	–	-517	–	–	–	–	–	–	–	40.91	8.36	
0137−0153	2,2′,4,6,8,10	4426	2.41	-193	218	1935	3125	–	8.2	5.	22.6	0.22	35.95	6.32	
0145+0416	2,2′,4,6,7,10	4588	3.96	626	1113	2341	–	22.5	12.5	–	–	–	33.1	5.36	
0146+0142	2,2′,4,5,7,10	5627	4.87	495	–	3038	4044	17.1	9.2	6.7	18.	0.37	–	7.24	
0226−1024	2,2′,4,5,7,10	7344	4.72	604	1861	3386	4507	26.5	7.4	4.3	24.6	0.17	54.12	6.21	
0335−3339	2,2′,4,5,7,9,10	7404	15.90	–	-77	599	–	26.2	1.7	7.7	–	–	95.66	14.16	a(.56)
0903+1734	2,2′,4,5,7,10	10433	4.34	-1350	–	1548	5630	25.3	4.7	4.5	26.5	0.17	–	4.9	
0932+5010	2,2′,4,5,7,9,10	6564	3.88	1597	3004	3619	5387	8.5	6.2	4.7	18.5	0.25	35.03	5.8	a(.33)
1011+0910	2,2′,4,6,7,9	4969	6.84	1861	2716	3232	3754	16.1	7.9	5.2	11.1	0.47	40.91	9.16	
1029−0125	2,2′,3,6,8,10	2023	2.22	-957	669	1645	3400	14.8	8.0	4.9	23.2	0.21	42.96	4.41	
1205+1436	2,2′,3,6,8,10	910	1.04	-876	-125	1412	4272	–	10.1	5.7	22.7	0.25	18.74	2.87	
1208+1535	2,2′,3,5,7,10	5277	4.64	-332	1842	2709	5222	16.3	6.3	2.3	24.	0.1	23.98	6.92	
1212+1445	2,2′,3,6,7,10	3799	6.05	-1805	-848	1741	2363	–	3.8	2.1	4.9	0.43	25.29	3.37	
1216+1103	2,2′,3,5,7,10	4996	4.66	46	530	2032	3055	–	13.7	7.1	27.5	0.26	19.37	3.71	
1231+1320	2,2′,3,5,7,9,10	5772	6.38	2469	–	2612	4492	5.5	7.5	8.2	18.6	0.44	42.59	7.19	a(.67)
1232+1325	2,2′,4,5,8,9	12792	1.84	671	–	3870	7123	18.2	17.5	4.9	42.9	0.11	58.76	11.8	
1235+0857	2,2′,3,6,8,10	1354	0.42	-536	–	1296	3840	20.5	10.4	5.5	24.	0.23	–	3.	
1235+1453	2,2′,3,6,8,10	2593	3.55	842	–	2941	3479	20.5	13.0	3.3	22.1	0.15	–	1.61	
1239+0955	2,2′,3,6,7,10	674	4.4	-859	766	1993	4327	24.4	7.1	2.	25.1	0.08	8.78	3.21	
1240+1607	2,2′,3,6,7,10	2391	4.47	479	–	2148	1570	26.6	16.8	3.7	26.9	0.14	33.8	2.96	
1243+0121	2,2′,3,5,8,10	5663	2.35	518	–	1916	2842	44.3	19.2	8.	41.8	0.19	–	4.95	
1246−0542	2,2′,4,6,7,10	4827	6.60	407	1750	1587	3699	12.9	4.8	8.6	20.1	0.43	44.29	4.21	
1303+3080	2,2′,4,6,8,10	2112	2.27	–	–	–	3879	–	–	4.8	21.6	0.22	16.94	3.8	
1309−0560	2,2′,4,6,7,10	4953	5.10	1543	3543	3812	5128	13.	8.1	6.	23.7	0.25	36.42	5.19	
1314+0116	2,2′,3,6,7,10	2337	7.41	138	–	1103	1672	21.7	16.1	–	17.9	–	–	2.26	
1331−0108	2,2′,3,5,8,9	8423	1.15	1441	1024	1935	3212	46.6	6.2	2.	13.8	0.14	18.07	6.95	

TABLE 2—*Continued*

Object	Samples	BI	DI	V (CIII]-CIV)	V (MgII-CIV)	CIV HWHM	CIII] HWHM	NV HREW	CIV HREW	AlIII REW	CIII] REW	AlIII/CIII]	2400 REW	2070 REW	Notes
1333+2840	2,2′,4,6,8,10	2247	2.2	680	-58	1432	–	35.5	19.9	–	–	–	29.86	13.31	
1413+1143	2,2′,4,5,8,10	7128	1.5	-270	–	1683	2937	32.9	18.8	4.6	35.	0.13	–	1.89	
1442–0011	2,2′,3,5,8,10	4971	2.83	670	–	3522	5481	28.2	14.6	2.3	20.	0.11	25.81	4.12	
1443+0141	2,2′,3,5,8,10	8983	3.26	343	–	2186	3102	13.8	8.5	9.2	28.8	0.32	72.37	7.98	
1641+4115	2,2′,4,6,8,10	2600	0.92	-173	1426	2128	7539	14.7	14.5	4.7	36.2	0.13	3.91	3.23	b
2154–2005	2,2′,3,6,7,10	1061	6.42	323	858	2438	3392	25.1	11.3	3.7	26.9	0.14	21.91	4.47	
2201–1834	2,2′,3,6,8,10	1176	2.19	-1947	-1899	4122	5442	16.8	7.5	3.	17.3	0.17	25.6	3.83	
2225–0534	2,2′,4,5,8,9,10	7694	0.48	-883	-528	1509	3251	25.3	11.3	8.1	43.4	0.19	53.38	7.67	a(.23)
2350–0045	2,2′,3,5,7,9,10	7328	5.08	-248	2178	1761	–	6.9	14.3	≤	–	–	54.78	5.71	a(.27)

[a] Fractional weights assigned to membership in Mg II–Al III BALQSO sample for mean spectrum.
[b] Al III upper limit.

between the continua of the non–BALQSOs and BALQSOs by simply co-adding the spectra comprising the various samples and displaying them. This avoids the necessity for subjective judgments about how to do the fitting. In order to do this, we must normalize the fluxes in some appropriate way.

We did this in an iterative procedure in which we first defined a window which appeared to be relatively free of either strong emission or absorption. After redshifting each object by the nominal redshifts of Table 1 and normalizing the flux in this window, we then inspected the co-added spectra comprising both the non–BALQSO and BALQSO objects. Examining these co-added spectra, it appeared that there were three rest-frame windows which were relatively free of strong emission or absorption even for the two extreme objects 0059−2735 and 0335−3339 and which occurred at minima of the ubiquitous Fe II emission. These windows are located at 1975–2000 Å, 2140–2155 Å, and 2190–2200 Å.

In order to minimize the effect of noise and weak intervening absorption features, we computed the median of the flux for every pixel which lay in any one of these windows, and normalized the spectra to that median value. We then co-added all these normalized spectra for the various subsamples defined. Prior to co-adding them, it was noticed that a few of the normalized spectra had very different spectral energy distributions from the rest, even in regions of the spectrum apparently unaffected by absorption troughs. By and large, these objects

TABLE 3

SUMMARY OF DEFINITIONS OF SAMPLES AND SUBSAMPLES

Sample Number	Definition	Text Reference
1	All objects having balnicity index 0	§ 4.1; Appendix A
1′.....	All objects having balnicity index 0, together with the two marginal objects 1234+0122 and 2211−1915	§§ 3.1, 4.1; Appendix A
2	All objects having balnicity index >0	§ 4.1; Appendix A
2′.....	All objects having balnicity index >0, except the two marginal objects 1234+0122 and 2211−1915	§§ 3.1, 4.1; Appendix A
3	All objects in sample 2′ which were found in the LBQS	§ 4.1
4	All objects in sample 2′ which were not found in the LBQS	§ 4.1
5	All objects in sample 2′ with balnicity index above the median value of sample 2′ (4970 km s^{-1})	
6	All objects in sample 2′ with balnicity index below the median value of sample 2′ (4970 km s^{-1})	
7	All objects in sample 2′ with detachment index above the median value of sample 2′ (3.71)	§ 4.2.3; Appendix B
8	All objects in sample 2′ with detachment index below the median value of sample 2′ (3.71)	§ 4.2.3; Appendix B
9	All objects in sample 2′ having a weight associated with Mg II/Al III broad absorption >0.0	§§ 4.2.3, 5.2
10	All objects in sample 2′ having a weight associated with Mg II/Al III broad absorption <1.0	§§ 4.2.3, 5.2

NOTE.—Objects with Mg II/Al III broad absorption weights which satisfy $0 < w < 1.0$ appear in both samples 9 and 10. See § 5.2.

TABLE 4

MEDIAN AND MEAN INDICES FOR SAMPLES

Index	Stat.	Sample All	1	1′	2	2′	3	4	5	6	7	8	9	10
No. Of Objects in Sample		71	29	42	31	40	23	17	20	20	20	20	6	34
V(CIII]-CIV)	median	323.69	368.56	299.54	138.84	323.69	-1.68	495.32	344.45	-59.19	344.45	-59.19	1441.68	46.83
	mean	279.93	495.09	448.08	125.46	143.59	-29.48	397.44	365.62	-66.75	293.70	-14.85	1611.02	-34.27
	RMS	941.36	910.55	901.24	944.15	963.15	995.16	885.33	888.05	1007.23	1082.10	820.30	755.12	829.68
V(MgII-CIV)	median	903.03	1101.62	1096.77	669.08	669.08	530.39	1113.42	765.13	669.08	1113.42	212.17	-77.76	669.08
	mean	1003.62	1222.11	1187.03	800.74	806.11	411.45	1266.53	937.31	709.89	1318.01	108.05	786.66	809.64
	RMS	1057.51	843.23	827.29	1203.42	1246.38	1045.44	1345.16	1161.21	1336.96	1233.09	908.77	1441.04	1246.04
CIV HWHM	median	2148.20	2554.63	2554.63	1935.32	1935.32	1935.32	1935.32	2032.08	1935.32	2032.08	1915.97	2612.68	1935.32
	mean	2355.48	2568.63	2525.28	2200.94	2216.96	2160.52	2294.56	2308.12	2125.79	2206.26	2228.84	2450.11	2181.63
	RMS	899.22	921.70	907.23	861.19	880.25	749.72	1055.10	922.86	850.59	900.22	883.39	1259.34	829.38
CIII] HWHM	median	3675.44	3502.67	3502.67	3753.98	3753.98	3400.57	3879.64	3856.07	3699.00	4044.56	3400.57	3753.98	3699.00
	mean	3741.14	3502.97	3540.25	3908.50	3901.85	3569.98	4399.65	4056.11	3756.16	3766.45	4029.72	4645.35	3805.91
	RMS	1246.78	1073.05	1056.40	1344.53	1374.25	1091.33	1631.63	1375.72	1396.28	1330.07	1441.00	1733.17	1325.43
NV HREW	median	18.90	17.60	17.60	20.50	20.50	20.50	22.50	22.90	20.50	17.10	20.50	18.20	21.70
	mean	19.97	18.21	17.89	21.38	21.86	22.40	21.17	23.17	20.38	18.50	25.64	22.52	21.74
	RMS	7.64	3.70	4.06	9.54	9.51	10.92	7.67	11.76	6.15	7.05	10.66	15.35	8.53
CIV HREW	median	9.20	9.40	9.40	8.20	8.50	10.10	8.10	8.50	10.10	7.50	10.90	7.50	10.10
	mean	10.53	11.17	10.83	10.07	10.29	10.71	9.71	10.14	10.44	8.48	12.30	8.14	10.62
	RMS	4.60	4.43	4.49	4.73	4.74	4.10	5.59	5.34	4.20	4.34	4.40	5.80	4.58
AlIII REW	median	4.50	4.00	3.70	4.70	4.80	3.70	5.00	4.90	4.70	4.70	4.80	5.20	4.70
	mean	4.56	3.99	3.93	4.96	5.06	4.59	5.69	5.64	4.45	5.01	5.11	5.60	4.97
	RMS	1.93	1.72	1.67	2.00	2.00	2.27	1.42	2.19	1.63	2.14	1.93	2.49	1.94
CIII] REW	median	21.60	21.20	21.10	22.70	23.20	23.20	22.60	24.60	22.60	20.10	23.20	13.80	23.40
	mean	22.38	20.95	20.63	23.39	23.79	22.66	25.48	26.16	21.54	20.29	27.09	21.60	24.07
	RMS	7.13	4.18	4.25	8.54	8.59	7.33	10.26	9.96	6.58	6.37	9.25	14.53	7.86
AlIII/CIII]	median	0.19	0.19	0.19	0.20	0.20	0.19	0.22	0.19	0.21	0.25	0.19	0.14	0.20
	mean	0.22	0.20	0.20	0.23	0.23	0.21	0.26	0.23	0.23	0.27	0.19	0.29	0.22
	RMS	0.11	0.10	0.10	0.11	0.11	0.10	0.12	0.11	0.11	0.14	0.06	0.19	0.10
2070 REW	median	4.68	4.33	4.33	4.90	4.90	4.12	5.80	5.80	3.80	5.19	4.12	8.36	4.41
	mean	4.99	4.39	4.36	5.41	5.48	4.54	6.77	6.45	4.52	5.64	5.33	9.60	4.76
	RMS	2.60	2.09	2.05	2.85	2.89	1.93	3.49	2.81	2.70	2.62	3.20	2.84	2.24
2400 REW	median	29.86	29.51	28.09	33.10	33.80	25.60	36.42	42.59	25.60	35.03	27.34	40.91	29.86
	mean	32.64	29.92	29.41	34.82	35.57	31.10	41.64	44.60	27.08	37.45	33.58	49.48	32.48
	RMS	15.71	11.45	11.22	18.30	18.59	15.44	21.25	20.62	11.59	19.53	17.95	26.08	15.49
Luminosity	median	43.28	43.26	43.27	43.32	43.31	43.28	43.59	43.51	43.26	43.42	43.28	43.57	43.28
	mean	43.34	43.27	43.28	43.38	43.38	43.32	43.47	43.44	43.32	43.41	43.36	43.56	43.35
	RMS	0.25	0.17	0.16	0.28	0.29	0.21	0.36	0.29	0.29	0.31	0.28	0.19	0.30
BI	median	-	-	-	4953.00	4970.00	3799.00	5082.00	6564.00	2337.00	4969.00	4426.00	7404.00	4588.00
	mean	-	-	-	4713.93	4948.85	4224.52	5928.82	7209.25	2688.45	4891.75	5005.95	8436.50	4333.38
	RMS	-	-	-	3051.21	2932.35	2886.26	2780.33	2210.71	1416.33	2361.78	3473.47	3070.06	2476.31
DI	median	-	-	-	3.71	3.71	3.26	3.96	3.26	3.55	4.87	2.20	1.84	3.55
	mean	-	-	-	4.08	4.02	3.61	4.59	4.24	3.81	6.03	2.02	5.55	3.75
	RMS	-	-	-	3.01	2.87	1.90	3.81	3.51	2.12	2.76	0.92	5.69	2.08

TABLE 5

K-S TEST RESULTS FOR VARIOUS INDICES AND PAIRS OF SAMPLES[a]

INDEX	SAMPLE PAIR (1, 2)	(1′, 2′)	(1′, 3)	(1′, 4)	(1′, 5)	(1′, 6)	(1′, 7)	(1′, 8)	(1′, 9)	(1′, 10)
V (C III] − C IV)	38.62	59.17	30.85	94.40	97.58	30.16	85.74	31.76	12.14	31.25
V (Mg II − C IV)	15.61	14.92	7.33	42.75	66.06	19.51	61.52	3.96	53.74	22.39
C IV HWHM	11.41	19.26	22.84	43.04	57.25	16.22	66.71	20.77	97.66	17.35
C III] HWHM	46.00	72.52	93.61	31.03	31.14	87.75	41.58	97.69	74.35	85.38
N V HREW	3.59	1.99	7.19	12.55	1.62	31.21	16.02	2.52	54.41	3.40
C IV HREW	11.41	19.26	22.84	43.04	57.25	16.22	66.71	20.77	97.66	17.35
Al III REW	10.40	3.19	69.33	0.24	3.11	31.94	47.49	1.58	17.77	6.79
C III] REW	26.74	19.48	23.83	31.03	4.55	37.09	71.53	8.05	44.13	10.63
Al III/C III]	78.61	93.53	98.74	80.30	83.03	85.82	17.68	86.12	64.01	90.12
2070 REW	53.50	37.76	97.76	13.30	3.79	81.19	40.90	60.12	1.40	91.06
2400 REW	63.23	42.06	70.45	5.43	2.99	95.38	41.14	77.82	2.35	85.11

NOTE.—REW and HREW are rest equivalent widths and half-rest equivalent widths (in angstroms).

[a] The entries in the table give the probability *in percentages* that the observed K-S statistic would be exceeded by chance for the index and pair of samples in question if the samples were drawn from the same parent population.

TABLE 6

ANALYSIS OF CORRELATION BETWEEN VARIOUS INDEX PAIRS FOR BALQSOs

Index 1	Index 2	Number of Objects	% Probability τ (+% Probability Spearman)[a]
BI	V (C III] – C IV)	37	7.11
BI	V (Mg II – C IV)	26	26.1
BI	C IV HWHM	38	30.2
BI	N V HREW	34	91.7
BI	C IV HREW	38	41.9
BI	Al III REW	35	10.6
BI	C III] REW	35	29.9
BI	2070 REW	40	0.0121 (0.03, 0.09)
BI	2070 REW	34[b]	0.508 (0.64, 0.46)
BI	2400 REW	33	0.0059 (0.03, 0.08)
BI	2400 REW	27[b]	0.0097 (0.044, 0.007)
DI	V (C III] – C IV)	37	14.3
DI	V (Mg II – C IV)	26	5.52
DI	C IV HWHM	38	88.0
DI	N V HREW	34	9.93
DI	C IV HREW	38	1.2 (1.2, 1.0)
DI	Al III REW	35	76.4
DI	C III] REW	35	1.0 (1.5, 1.3)
DI	2070 REW	40	51.4
DI	2400 REW	33	11.7
2400 REW	2070 REW	63	0.357 (0.34, 0.27)
2400 REW	Al III REW	56	0.272 (0.34, 0.28)
Luminosity	V (C III] – C IV)	67	27.4
Luminosity	V (Mg II – C IV)	54	11.5

[a] The first number in this column is the *percentage* probability that a value less than the observed value of the Kendall τ statistic would occur by chance among uncorrelated indices. The numbers in parentheses give the corresponding probabilities for the Spearman d and Spearman rs statistics.

[b] Mg II BALs removed.

turned out to be BALQSOs which had either Al III or Mg II absorption troughs or both. Figures 3*a*, 3*b*, and 3*c* show the mean spectra for samples 1′, 9, and 10—that is, the non–BALQSOs (including the two marginal objects), the BALQSOs having low-ionization troughs, and those not having low-ionization troughs.

There is naturally some ambiguity about which objects to include in sample 9. We comment on this below. Figures 3*a*, 3*b*, and 3*c* also show the rms deviations about the mean for each of these three samples. Figure 3*d* shows the comparison of the mean spectra based upon these three samples. Inspection of the spectra in Figure 3 makes two things apparent. First, there is a striking difference between the continua of the BALQSOs with low-ionization troughs compared with both the BALQSOs with only high-ionization troughs and the non–BALQSOs. Between about 1550 and 2000 Å the continua of the Al III/Mg II BALQSOs are relatively flat (with the flux plotted per unit wavelength), whereas the remaining objects rise toward the blue. Second, redward of 1550 Å there is virtually no difference in either the continuum shape or spectral features between the high-ionization BALQSOs and the non–BALQSOs.

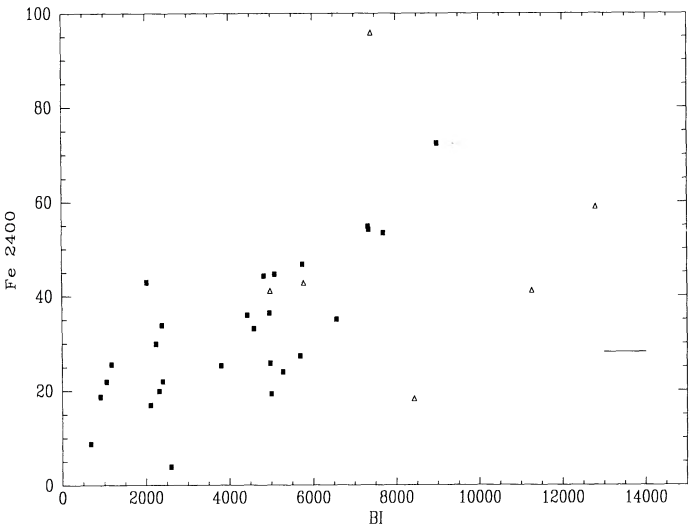

FIG. 2.—Correlation of the Fe II λ2400 index with the balnicity index for all the objects in sample 2′. The open triangles are those objects with a Mg II BALQSO weight greater than or equal to 0.5. The short line is the median strength in the non–BALQSO sample 1′.

Shortward of 1550 Å there does appear to be a general decrease in the flux of the BALQSOs relative to the non–BALQSOs, but in the summed spectra it is very difficult to disentangle such an effect from the effect of the absorption troughs. The comparison of the summed spectra of the high-ionization–only BALQSOs and non–BALQSOs reinforces the conclusion drawn from § 4 concerning the subtlety of any differences between BALQSO and non–BALQSO emission-line properties.

Measurement of the same indices defined in § 3 could be made for the summed spectra, but the same uncertainties arise in placing the continuum, especially for the N V and C IV indices, so that this is not an especially useful exercise. However, we have measured the Mg II properties in samples 1′ and 10 (sample 10 being the BALQSO set least affected by Mg II absorption). The two profiles are virtually indistinguishable. They are both characterized by a very broad and fairly symmetrical component extending to $\pm 13{,}000$ km s^{-1} from the line center. The equivalent width of this component, which

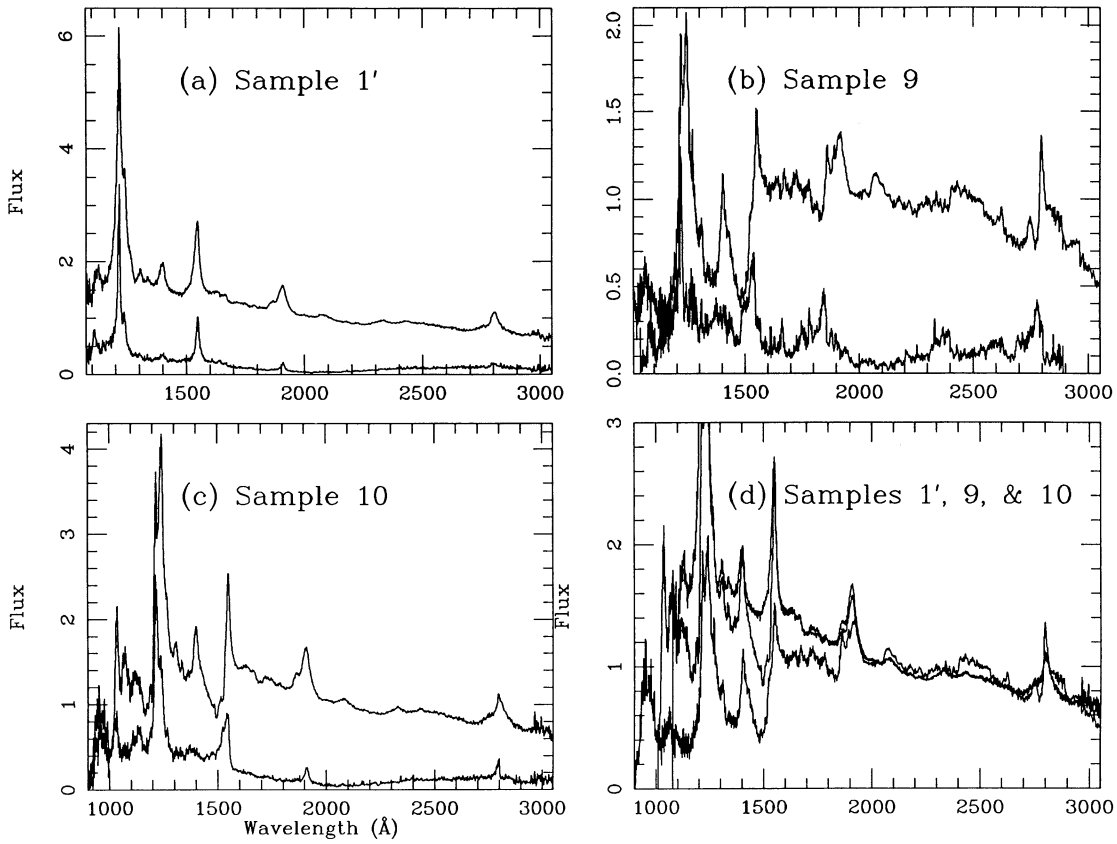

FIG. 3.—Panels *a*, *b*, and *c* are the averaged spectra and the associated rms values for samples 1′ (the non–BALQSO sample), 9 (the Mg II–Al III BALQSOs), and 10 (the BALQSOs without noticeable Mg II or Al III absorption troughs), respectively. Panel *d* superposes the three averaged spectra, which have all been normalized to unity at about 2000 Å. Note that at the scale of panel *d* samples 1′ and 10 are indistinguishable longward of the C IV absorption trough at about 1550 Å.

involves an unknown contribution from Fe II, is 34 Å for sample 1′ and 38 Å for sample 10. Superposed on this broad component is a core. If we draw a flat effective continuum across the base of this core, the equivalent width of the core is 9 Å for both spectra and it has FWHMs of 3200 and 2800 km s^{-1} for the sample 1′ and sample 10 spectra, respectively.

The region of the Al III–C III] lines is of special interest. Our individual measures and the accompanying K-S tests suggested some significant differences between the Al III in some samples, and weaker evidence for differences in C III]. We found no evidence from the K-S test for enhancement of the Al III/C III] ratio. Inspection of the spectra of Figure 3*d*, when plotted at a suitable scale, supports the evidence that there is some small enhancement of flux in the Al III–C III] region in the BALQSOs.

Instead, in Figure 4 we display the Al III–C III] region in a slightly different way. We take the difference between the BALQSO and non–BALQSO mean spectra and divide this difference by the fit to the continuum of the non–BALQSOs. The spectrum in Figure 4 can thus be interpreted as the difference in equivalent widths between the two samples.

Three things are noteworthy about Figure 4. First, the excess flux in the vicinity of the Al III–C III] blend is a broad feature which extends from about 1815 Å to about 1970 Å. Comparing it with the extent of the Al III–C III] emission in the sample 1′ mean spectrum does suggest that Al III and C III] are involved, since these two features can be traced out to about these same wavelengths. On the other hand, there is no suggestion that the excess flux is a blend of two components, but it appears rather as a single smooth feature whose peak occurs at about 1895 Å. However, the signature of the blend is obvious in the two mean spectra from which this difference spectrum was formed, so that we have not blurred out the blend by the process of forming the two mean spectra. Moreover, there is an adjacent region of weaker but obvious excess flux extending from about 1700 to 1800 Å. These latter two properties argue that this excess flux is not due to Al III and C III] but may be due to Fe II or Fe III. The composite spectrum of Francis et al. (1991) clearly shows a broad complex of emission underlying the Al III–C III] blend.

Second, the region from 2000 Å to about 2650 Å in Figure 4 is remarkably flat, and the 2070 Å feature and broad Fe II complex from 2250 to 2650 Å have almost completely disappeared. If the excess flux discussed above is real and is due to Fe II, this suggests that some special excitation mechanism is at work which singles out the multiplets in the 1700–1970 Å region. In drawing the local continuum prior to deblending the Al III–C III], some of this excess was probably removed and what remained may have provided a greater percentage contribution to the Al III than to the C III].

Third, Figure 4 shows a *deficit* of flux increasing from about 1700 Å to the C IV emission line, shortward of which the BALQSO mean spectrum, and hence the difference spectrum, is dominated by the C IV absorption trough. This flux deficit could be an artifact in the construction of the two mean spectra, though we cannot think of any reason why this should

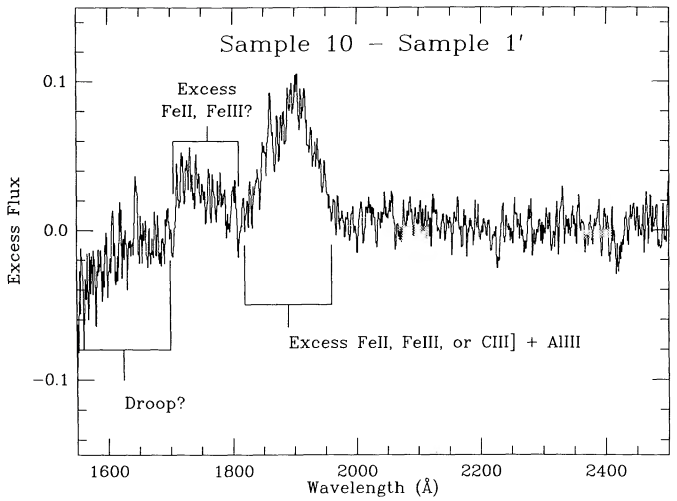

FIG. 4.—Difference spectrum resulting from subtracting the average spectrum of sample 1′ from that of sample 10. The excess emission in the region from about 1820 Å to about 1960 Å represents about a 3 σ excess. If real, it could be due to C III] + Al III, but the shape of the excess and the location of its peak suggest that it is not C III] + Al III. It may be due to Fe II or Fe III, as may the excess from about 1700 to 1800 Å. The "droop" from 1550 to 1700 Å is discussed in the text.

be. It is also conceivable (but we think most unlikely) that this BALQSO flux deficit, if real, is due to C IV absorption from *infalling* gas in the BALQSOs. It could also involve a deficit in the broad component of the red wing of the C IV emission line itself relative to the non–BALQSOs, perhaps because of orientation effects. Examination of the entire difference spectrum suggests to us, however, that a small difference in the continuum between the high-ionization BALQSOs and the non–BALQSOs exists shortward of about 1700 or 1800 Å all the way down to N V. This could be merely a milder manifestation of the effect seen in the low-ionization BALQSOs as described below. It seems unlikely that this continuum difference is due to reddening, because it sets in so suddenly, but this possibility needs to be investigated. Possibly it is associated with differences in the effective temperatures of accretion disks viewed preferentially at different angles.

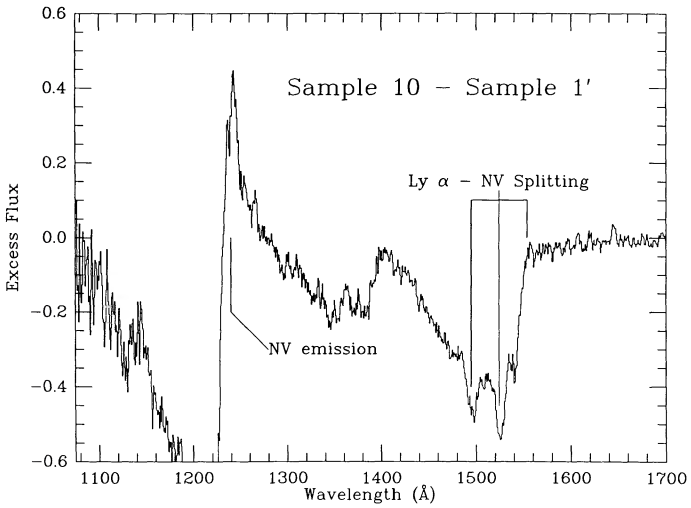

FIG. 5.—Same difference spectrum as in Fig. 4 in the region covering the N V and C IV emission and absorption features. The excess N V emission in the BALQSO sample 10 is evident. This excess flux represents an equivalent width excess of at least 5 Å and has a formal significance of about 3 σ. The two minima in the C IV absorption trough have a velocity splitting very nearly equal to the velocity difference between Lyα and N V, and the lower velocity minimum of the two is itself displaced by about this same amount from zero velocity.

In Figure 5 we show a portion of the difference spectrum in the region of the C IV and N V troughs. Two things are noteworthy about Figure 5. First, there is the appearance of structure in the C IV trough, which involves about 36 BALQSOs. It may be significant that velocities at the strong minima are about equal to and double that of the N V–Lyα separation. A similar coincidence was noted by Turnshek et al. (1988) in connection with their studies of three BALQSOs with P Cygni–like profiles. Note that other structure which involves only velocity *differences* and not the absolute velocities would of course be washed out in this composite spectrum (cf. Braun & Milgrom 1989).

Second, there appears to be an excess amount of flux in N V, despite the possible general deficit of flux shortward of the C IV emission. *The existence of this excess is not influenced by the choice of continuum*, though its interpretation in terms of the equivalent width of N V is. We have measured directly the excess N V in the difference spectrum represented by Figure 5 by simply drawing a "continuum" which is flat at zero. This is probably a lower limit to the N V equivalent width difference, because, as noted above, there may be a flux deficit associated with a continuum deficit as well. We find this lower limit to the excess N V equivalent width to be 5.0 Å, which agrees very well with the results obtained from the measurement of the individual spectra.

We have attempted to estimate the statistical significance of some of these differences between the mean spectra. In the case of the difference between the mean spectra of sample 1′ and sample 10 in the region around Al III and C III], we computed the means and the dispersions for the combined equivalent widths of Al III and C III] in these two samples. The expected dispersions in these two means are of the order of the dispersion in each sample divided by the square root of the number of objects in that sample. The square root of the sum of the squares of these dispersions of the means is our estimate of the uncertainty in the strength of the difference spectrum arising from the scatter in the emission-line strengths of the objects making up the two samples. This number turns out to be about 1.6 Å. The equivalent width of the feature in the difference spectrum is about 5 Å, so that we consider the reality of this excess to be about a 3 σ result.

We estimated the significance of the N V excess in exactly the same way we did for the excess flux in the region of the Al III–C III] region, with similar results: the dispersion for the difference of the mean N V strengths for these two samples is about 1.6 Å, so that a 5 Å difference in excess flux is a 3 σ result. In fact, the N V difference is probably substantially more significant than this because a sizable portion of the dispersion in the set of N V indices certainly arises from uncertainties in placing the continuum for the individual objects.

5.2. *The BALQSOs with Low-Ionization Troughs*

As described above, the set of BALQSOs which showed obvious Al III and/or Mg II absorption troughs stood out at once as having anomalous continua. We have therefore formed a subsample of BALQSOs which display this characteristic. Just as there are ambiguities in deciding whether to place a given QSO in the BALQSO or the non–BALQSO sample,

there are ambiguities in deciding whether some BALQSOs have Al III or Mg II absorption troughs. In the case of the BALQSOs in general, we were guided by the formulation and measurement of the balnicity index. Ultimately, it would be desirable to formulate a related index to measure the strength of the low-ionization troughs.[6] This might involve formulating balnicity indices specifically for Al III and Mg II and then taking the ratio of these indices to the C IV balnicity index. The complexity of the Fe II emission and absorption makes locating a continuum very difficult, and it is often not clear whether a given feature is a low-ionization trough or a gap between emission, and we have not attempted such a procedure. Instead, three of us independently examined all the spectra and assigned subjective weights of 0, $\frac{1}{3}$, $\frac{2}{3}$, and 1 to every BALQSO, corresponding to descriptions of "little or no evidence for low-ionization troughs," "possible," "probable," and "certain" low-ionization troughs. The averages of these weights were then used. The average weights for membership in the Mg II–Al III BALQSO sample which have nonzero values are indicated in the "notes" column of Table 2. The mean spectrum for sample 9 was formed by multiplying each BALQSO by this average weight before forming the mean, and the mean spectrum for sample 10 was formed by multiplying each BALQSO by one minus this weight.

The reality of the difference between the flux distributions of the low-ionization BALQSOs and both the "normal" BALQSOs and the non–BALQSOs seems apparent from Figure 3*d*, but since the mean spectrum of the low-ionization BALQSOs involves only nine objects, it is desirable to confirm this quantitatively. Since *weighted means are involved in the spectra of Figure 3d*, the K-S test is not directly applicable, and in any case, in view of the small sample size of the low-ionization BALQSOs, we used a different approach from that used above. We defined a "1600 Å index" to be the integrated flux between 1600 and 1775 Å. We measured this index for a mean spectrum formed by combining the non–BALQSOs and those BALQSOs which had a Mg II weight of zero—i.e., those that showed no sign of low-ionization troughs. There are 62 objects in this sample. We also measured this index for the weighted mean spectrum associated with the nine BALQSOs which had nonzero Mg II weights. We then ran Monte Carlo simulations in which nine objects were randomly selected from the combined set of 62, and the same set of nine weights associated with the low-ionization BALQSOs randomly assigned to these nine objects. From this "pseudo–low-ionization BALQSO" sample, a mean spectrum was formed and its 1600 Å index measured. Out of 100,000 trials we found one case in which the index from one of these pseudosamples differed from that of the mean of the 62 by an amount greater than did the actual low-ionization BALQSO sample. This is strong evidence that the differences in the spectral energy distribution between the low-ionization BALQSOs and the other objects shown in Figure 3*d* are real.

Tables 3 and 4 suggest enhancement for both the Fe II $\lambda\lambda$2070 and 2400 indices of sample 9, though not for the indices involving Al III and C III]. However, Figure 6 shows a region of the spectrum in the vicinity of Al III–C III] and shows the striking difference between the low-ionization BALQSOs and the non–BALQSOs.

[6] It should be stressed that what we are calling "low-ionization BALQSOs" always have the usual, and sometimes exceedingly strong, high-ionization troughs due to C IV and N V, in addition to the low-ionization troughs.

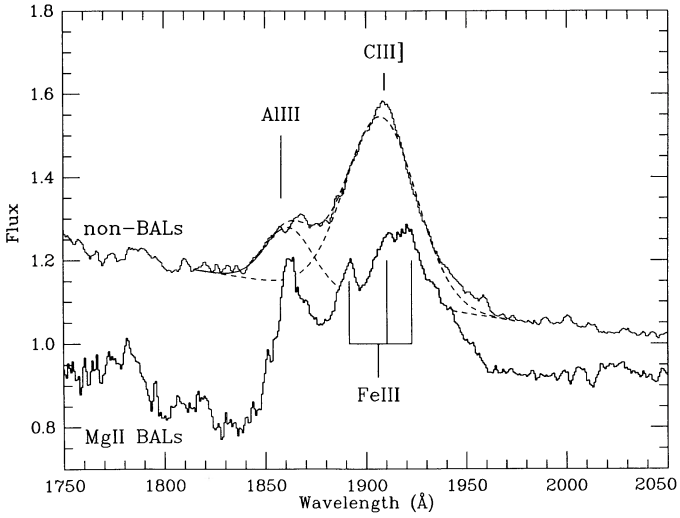

FIG. 6.—Comparison of the non–BALQSO (sample 1′) average spectrum with the Mg II–Al III BALQSO (sample 9) average spectrum in the region of the Al III–C III] features. The BALQSO spectrum has been displaced downward by 0.1 unit. In the non–BALQSO spectrum we also show the results of deblending the Al III and C III] features using the algorithm described in the text. The locations of the three lines of Fe III from multiplet UV 34 have been shifted by 600 km s^{-1} to the blue from their laboratory values.

There is, in fact, no convincing evidence for any emission peak at the expected position of C III]. In fact, the mean low-ionization BALQSO spectrum shows a strong resemblance to a broadened spectrum of 0335 − 3339, even though 0335 − 3339 contributes only 9% to the weighted mean low-ionization BALQSO spectrum. In particular, this spectrum has peaks at approximately 1892, 1912, and 1920 Å. HB gave convincing arguments that in 0335 − 3339 these peaks should be identified with Fe III. There is also a strong peak due to Al III at 1862 Å whose width and centroid are probably affected by the Al III absorption in this sample. The strong difference in the structure of the emission in this region of the spectrum between the Mg II BALQSOs and the other objects in the sample probably vitiates our simple two-component deblending algorithm.

We speculate on the nature of the low-ionization BALQSOs in § 6.

6. SUMMARY AND DISCUSSION

6.1. *Summary of Main Results*

Analysis of our various samples has yielded the following results:

1. We find no statistically significant differences in the emission-line characteristics between non–BALQSOs and BALQSOs *when the BALQSOs are restricted to those found in the LBQS.*

When the *full* set of BALQSOs, or special subsamples thereof, are considered, there appear to be some statistically significant differences, though it must be admitted that the estimates of the significance are not always as robust and secure as one would like. In particular:

2. There is enhancement of the equivalent width of the red half of the N V emission in BALQSOs over that in the non–BALQSOs. This enhancement amounts to about 5 Å, i.e., to an increase in equivalent width of about 25%. This excess is found both in the measurement of individual objects and in the difference of the set of mean spectra. We find no correlation of the

N v emission strength with either the balnicity index or the detachment index. The fact that the N v excess was found only in the full sample and not in the LBQS sample we interpret as meaning that the statistical significance of the excess, as measured by the K-S test, is only strong enough to be detected in the full sample, but not in the LBQS BALQSO or non–LBQS BALQSO samples separately.

3. In contrast to the case of N v, there is no clear excess in the Fe II $\lambda\lambda$2070 and 2400 indices in either the LBQS BALQSOs or the non–LBQS BALQSOs, but the Mg II BALQSOs show evidence for an excess. However, there is a strong correlation between these two indices and the balnicity index. The correlation persists when the Mg II BALQSOs are removed from the sample.

4. There appears to be a very small amount of excess flux in the high-ionization–only BALQSOs compared with the non–BALQSOs in the region around the Al III–C III] blend. This excess is more likely due to Fe III (or Fe II multiplets in which some special excitation mechanism is operating) than to Al III and C III].

5. There is some evidence for an anticorrelation between the C IV and C III] strengths and the degree of detachment of the C IV absorption trough, in the sense that strong emission does not accompany detached troughs.

6. There is a large velocity shift between the C IV peak and the Mg II peak and probably a much smaller one between the C IV and C III] peaks, and the two shifts are correlated. We find no convincing evidence for differences in velocity shifts between the BALQSOs and the non–BALQSOs.

7. There is some evidence that systematic structure occurs in the C IV absorption troughs, with two minima being present and having velocities about equal to and twice that of the separation between Lyα and N v. We have not attempted to evaluate the statistical significance of this result. Our sample represents about a third of all BALQSOs known to us which have observable C IV. The best way of confirming this result will be to compile a mean spectrum from data of comparable quality from the remaining BALQSOs. If this structure is confirmed, it is obviously a strong indication that radiative acceleration is an important factor in the dynamics of the BAL clouds.

8. There is very little difference in the continuum between the high-ionization BALQSOs and the non–BALQSOs, though the BALQSOs may be very slightly redder in the region 1550–1700 Å, and this may persist shortward of C IV.

9. The subset of BALQSOs which show definite signs of Al III and/or Mg II absorption troughs differ most strongly from the non–BALQSOs. They have strong Fe II emission, show fairly convincing evidence for Fe III at a strength which dominates any underlying C III], and are distinctly redder than both the non–BALQSOs and other BALQSOs shortward of 2000 Å.

6.2. *Discussion*

We have stressed that one of the most significant results we have obtained is to demonstrate how similar BALQSO and non–BALQSO spectra really are aside from the absorption troughs themselves. We (and previous workers) have also stated that this would be an argument in favor of the "single population but different orientation" model as opposed to the "two population" model. How clean a distinction can be made between these two models, and how would we distinguish them conceptually?

Imagine that we could observe a large sample of optically selected QSOs from all possible orientations. (If there is an aspect dependence to the continuum, we would want to sample in such a way that we measure a set of objects within a given range of total luminosity, integrated over direction.) We could then measure the C IV balnicity index in each direction and for each object define a covering factor as the fraction of 4π steradians over which a nonzero balnicity index was obtained.

If the resulting distribution had a large delta function at a covering factor of zero (i.e., a significant fraction of QSOs simply had no BAL clouds at all) and a secondary maximum in this distribution at a moderately large covering factor, then there would be no question but that two separate populations of objects were involved. Even if there were a large maximum at a very small, but nonzero, covering factor and a second maximum at a much larger covering factor, we would still consider that two separate populations were involved. (Recall that the integral of the product of the covering factor with this distribution function must equal the observed fraction of QSOs which are BALQSOs, if the sample is indeed selected isotropically (cf. Morris 1988). As a practical matter, it seems unlikely that two closely spaced maxima in this distribution would occur, so that, conceptually, we may consider that *two different populations of QSOs are involved if there are two maxima in the covering factor distribution function.*

It would not be unreasonable to suppose that these two populations would have different emission-line characteristics. Had we found differences which were so marked that neither appeals to anisotropy of the emission nor the covering factor selection effect (discussed below) were plausible, then this would have been a strong argument for the two-population model. However, the converse is not true, as it is possible to construct plausible scenarios in which two populations would be involved whose BELR properties were indistinguishable. An example of such a model might be QSOs which find themselves in nuclei of higher than normal gas and dust density, either because of their youth (e.g., Low et al. 1989; Hazard et al. 1987) or because of some property of the host galaxy (e.g., a high supernova rate, whose ejecta Hazard 1989 has suggested might give rise to the broad absorption). While these QSOs might therefore be prone to show broad absorption, they could certainly have broad emission line regions indistinguishable from the non–BALQSOs. Therefore, our result that the degree of emission-line differences between BALQSOs and non–BALQSOs is small is *consistent* with the single-population model but does not *demand* it. To do that requires some independent way of estimating the covering factor distribution function, and that in turn involves appeal to scattering models (Junkkarinen 1983; Hamann, Morris, & Weymann 1990).

We favor the single-population model for the general class of BALQSOs because of the absence of strong emission-line differences between BALQSOs and non–BALQSOs together with the limits to the covering factors inferred from scattering models. An additional argument in favor of the single-population model comes from the correlation we have found between the balnicity index and the Fe II emission strength together with the near-equality in Fe II emission strength between the non–BALQSOs and the BALQSOs, especially when the Mg II BALQSOs are excluded from the BALQSOs. The balnicity index–Fe II correlation points to some causal connection between the production of the broad absorption and the Fe II emission. In the two-population supernova ejecta scenario mentioned above, for example, one might speculate

that the higher the *current* supernova rate, the more BAL clouds and the more Fe-rich material are available to enhance the Fe II emission. But then in the other population, where the *current* supernova rate is very much lower, the near-equality in Fe II emission-line strength has no natural explanation and has to be considered a coincidence.

In fact, we have established that there *are* small differences in the emission-line properties between the BALQSOs and the non–BALQSOs, and the question is whether emission anisotropies and the covering factor bias *can* plausibly account for these differences. We give only a very brief and qualitative discussion here. A more detailed discussion will be presented elsewhere (Hamann et al. 1990).

Before beginning this discussion, we outline the (admittedly rather ad hoc) picture we have for the nature of the BALQSOs and their relation to radio-loud and radio-quiet QSOs:

i) There is some evidence that the distribution of radio power in high-redshift, luminous QSOs has a minimum around $\log R \approx 0.5$–1.5 (Visnovsky et al. 1990).

ii) As noted in § 1, the evidence is accumulating that the BALQSO phenomenon does not occur among radio-loud sources.

iii) The radio data on both BALQSOs and non–BALQSOs (Stocke et al. 1990; Visnovsky et al. 1990) are consistent with the speculation that the value of $\log R$ at which the minimum in the distribution occurs is about the same value of $\log R$ above which the BALQSO phenomenon disappears.

These points suggest that we are dealing with two different populations of objects, in one of which, the radio-loud QSOs, kinetic energy is channeled into a sharply collimated relativistic beam of plasma. In the other population, such sharp collimation does not take place (perhaps because of different properties of the accretion disks), but a comparable amount of kinetic energy appears instead as a poorly collimated subrelativistic wind (see also Boroson, Persson, & Oke 1985). What we have termed the intermediate radio strength sources may either represent a transition in properties of individual objects or simply an overlap between the two populations.

In the remaining description of the picture we have of the BALQSO phenomenon, we consider only the radio-quiet population.

iv) As is now widely believed to be the case for Seyfert galaxies (cf. Antonucci & Miller 1985), we suppose that a large "obscuring torus" of dense, low-ionization gas (and possibly dust) surrounds the nucleus. The dimensions of this torus are large compared with those of the broad emission line region responsible for the bulk of the Lyα emission.

v) A combination of thermal wind and radiation pressure causes clouds to be ablated off the top and bottom surfaces of this torus. The more powerful the wind, the larger and more numerous the clouds. These clouds begin to be accelerated by the wind.

vi) The clouds just described break up into a hierarchy of smaller and smaller clouds which are accelerated to higher and higher velocities. It is these smaller fragments which are responsible for the optically thin and highly ionized absorption troughs. In passing we remark that we are aware that there are objections to such a picture based on linear theories of various hydrodynamic instabilities. Nonetheless, the profiles of the troughs (cf. Fig. 5) strongly suggest to us a hierarchical process of this type. We believe that the fate of such clouds in the nonlinear regime is not yet understood.

Note that in this picture the likelihood of intercepting the BAL clouds is greatest when the QSO is viewed from an angle which skims the surface of the torus. This is contrary to the usual presumption that ejection of the material occurs along polar jets, a view that has been espoused recently by Barthel (1990) by analogy with the "unified model" of radio-loud active galactic nuclei (AGNs): in the radio-loud AGNs, there appears to be a correlation between the strength of the optical Fe II emission and the orientation of the AGN in the sense that the strongest Fe emission appears to be associated with compact, flat spectrum sources which are thought to be seen "pole-on" (Steiner 1981; Boroson et al. 1985). At present we are aware of no other arguments in favor of either the "pole-on" or the "edge-on" geometry for the BALQSOs.

The fact that N V and Fe II have such different atomic properties, as well as the fact that the statistical natures of these two emission-line excesses seem different (not correlated with the balnicity index in the case of N V and strongly correlated with it in the case of Fe II), argue that different factors are at work to produce these two excesses.

Consider first the case of N V. Morris (1988) recently pointed out that if a sample of objects with a distribution of BAL covering factors is sampled, then those which are observed to be BALQSOs will have, on average, larger covering factors than those which are observed *not* to be BALQSOs. If there is a correlation between the BAL covering factor and the strength of some particular emission line, then that line will be enhanced in the BALs. The case of N V is especially favorable in this regard because a substantial amount of N V production might occur in the BAL region itself, partly from collisional excitation but also from scattering of continuum photons and more important, Lyα photons created in the BELR (Turnshek 1984a). This contribution to the N V emission from the BALR will be directly proportional to the covering factor. Whether this model can account quantitatively not only for the magnitude of the effect but also for the line profile of the Lyα and N V complex remains to be seen (Surdej & Hutsemekers 1987). A possible difficulty that has been raised with this explanation is that one also expects C IV to be enhanced in the BALR by both collisional excitation and continuum scattering, but not, of course, by Lyα scattering. We do not observe any enhancement. This might be because the ratio of the amount of N V produced in the BALR to that produced in the BELR is significantly larger than the same ratio for C IV, in part because of the N V augmentation in the BALR by the Lyα scattering. The enhancement of the C IV in the BALR may thus be too small for us to measure. In addition, as discussed in § 3, our C IV index may not include much of the contribution from the BALR if it is distributed over the underlying broad emission wings.

The enhanced Fe II in the objects with strong balnicity index is more difficult to understand. The correlation of Fe II strength with balnicity index was perhaps the most unexpected result of our analysis. There is still no argument on whether energy input by photoionization can account for the very large amount of energy released by the Fe II in AGNs in general, or whether some other mode of energy deposition is at work (cf. Francis et al. 1991; Netzer 1988; Joly 1988). Nor is there agreement on whether Fe II is produced in the same region as the high-ionization lines of the BELR or in a completely separate region.

In terms of the picture of the BALQSO geometry sketched above, we speculate that large clouds ablated off the torus would produce strong Fe II emission due to the shielding pro-

duced by the expected large column density of H I. As described above, the interaction of such massive clouds with a wind might produce debris which gives rise to broad absorption troughs having significant optical depths in C IV extending to high velocities. This is turn produces a large balnicity index and hence the correlation we have found. The interaction of the wind with these clouds might also be a source of additional energy input which may be required to explain the Fe II emission.

6.2.1. *The* Mg II *BALQSOs*

The Mg II–Al III BALQSOs pose especially interesting problems. In addition to the characteristics summarized in item 9 in § 6.1, recent work by Low et al. (1989) suggests that the Mg II BALQSOs may have unusual infrared properties as well.

Low et al. studied the properties of 11 QSOs which were selected from the *IRAS Point Source Catalog* on the basis of having "warm" [i.e., $F(25\ \mu m)/F(60\ \mu m) \geq 0.25$] *IRAS* colors, and compared them with the Palomar-Green (PG) sample. Some of the relevant conclusions were the following:

a) The *IRAS*–selected sample and the PG sample showed considerable overlap in their spectral energy distributions, but the *IRAS* sample had both somewhat higher median values of IR/optical flux and smaller $F(25\ \mu m)/F(60\ \mu m)$ ratios than the PG sample.

b) There was no obvious sign of increased reddening in the optical spectra with increasing IR/optical flux ratio.

c) Some tendency was noted for the strength of the Fe II emission (these were the optical transitions, not the UV Fe II transitions we have studied) to correlate with the IR/optical flux ratio.

d) Of the six *IRAS*–selected QSOs which were studied spectroscopically and which had redshifts high enough for Mg II to be accessible, two showed Mg II broad absorption.

e) Subsequently, an additional one of these 11 sources (which had been suspected to be a Mg II BALQSO) was confirmed by *IUE* spectra to be a Mg II BALQSO (Cutri 1990).

Thus, three out of seven *IRAS*–selected QSOs in which a Mg II BAL could have been detected turned out to be Mg II BALQSOs. This is a remarkably high incidence of Mg II BALQSOs. Using the value of 9% for the *apparent* fraction of optically selected QSOs which are BALQSOs (i.e., before applying a differential *k*-correction to get the true fraction—cf. Foltz et al. 1990) and using our weighted average of 6.06/40.0 ~ 0.15 as the *apparent* fraction of BALQSOs which are Mg II BALQSOs, we expect about 1.4% of all optically selected QSOs to be Mg II BALQSOs. (Of course the objects in the sample we have studied are high-luminosity, high-redshift objects. However, this fraction is consistent with the fraction found during preliminary inspection of about 350 spectra of LBQS QSOs in the redshift range 0.3–1.0 which are somewhat closer in luminosity to the Low et al. sample.) The a priori probability of finding three or more Mg II BALQSOs out of a sample of seven QSOs if the true probability is 0.014 is only 9.2×10^{-5}. This suggests that even though the mean IR and IR/optical properties of the *IRAS*–selected sources differed only moderately from those of the optically selected PG samples, they nevertheless acted to favor the selection of the Mg II BALQSOs. However, before too much effort is expended on explaining this result, it should be noted (Cutri 1990) that in a subsequent investigation of 16 QSOs found in the *IRAS Faint Source Catalog* (and using the same IR color criterion as for the *IRAS Point Source Catalog*) only one of the 13 objects which had redshifts high enough for Mg II to be accessible was a Mg II BALQSO. Moreover, this object was one of five which were also in the sample studied from the *IRAS Point Source Catalog*. Whether we are being misled by very small number statistics or whether there are real differences in the spectroscopic properties of the Point Source and Faint Source samples is not yet known.

In either case, the results of Low et al. (1989) suggest an intimate connection between the production of Fe II emission and the presence of strong IR emission, presumably from warm dust. This, together with the strong correlations which we have found between the Mg II BALQSOs and the Fe II emission strength, and the balnicity index and the Fe II emission strength, suggests the following possibility: in those BALR clouds which have both very high column densities and high physical densities (implied by the Fe III/C III] ratio in the Mg II BALQSOs as well as in the production of Fe II and Fe III absorption from excited states in 0059−2735; Hazard et al. 1987) dust can form, and survive. In our picture, it seems likely that the dust was preexisting, but when the clouds are ablated off the torus, the dust is exposed to a more intense radiation field and becomes warmer.

It will be very interesting to investigate all the known Mg II BALQSOs to see whether the apparent Fe II enhancement among the Mg II BALQSOs persists and, ultimately, to see whether the IR properties of these objects differ from those of the high-ionization BALQSOs and from the non–BALQSOs.

Can we construct a "single population" model to account specifically for the Mg II BALQSOs, or must we invoke a "two population" model? The answer will depend upon what future observations reveal about whether and how the infrared properties of the Mg II BALQSOs differ from QSOs in general, and on the extent to which the Mg II BALQSOs are much redder in the optical and near-IR than the typical QSO.

If Mg II BALQSOs ultimately turn out to have far-infrared colors which differ from those of the typical QSO, then we will almost certainly be driven to the two-population model, since it seems likely that the far-IR emission is emitted isotropically. In such a case, we might be able to construct a two-population model for the Mg II BALQSOs, where only the objects falling at the very high end of the column-density distribution of BALQSOs develop Mg II absorption and associated Fe II emission and warm dust. As a specific numerical example, a small fraction of all QSOs (e.g., 5% or 6%) could have substantial (e.g., 25%–30%) Mg II covering factors and the remainder have very small or zero Mg II covering factors. Covering factors as high as 25%–30% for a small number of objects may still be consistent with scattering models. We should then expect that for every Mg II BALQSO there should be two or three non–BALQSOs having comparable IR colors. In this model the large IR/optical flux ratio could simply be due to excess warm dust.

Alternatively, if there turns out *not* to be a clear distinction in the far-IR colors between Mg II BALQSOs and non–BALQSOs but a distinction in the IR/optical flux ratio is confirmed, then one might still construct a model in which all QSOs have roughly the same, but a rather small, Mg II covering factor, and only a very restricted range of lines of sight produce the Mg II BALQSO phenomenon. We would then have to appeal to orientation effects—through altered effective temperatures of the continuum and/or through actual extinction by dust—to raise the IR/optical flux ratio. The evidence in

this regard is still mixed: we found clear indications of redder continua in the Mg II BALQSOs shortward of about 2000 Å, whereas Low et al. (1989) found no indication of reddening as a function of the IR/optical flux ratio. If there is substantial reddening of the UV and optical continuum, there will then be substantial differential *k*-corrections between Mg II BALQSOs and non–BALQSOs, and this needs to be taken into account in calculating the fraction of QSOs which are Mg II BALQSOs as a function of redshift (cf. Foltz 1990). Finally, in this model we would also have to contrive a way to make the Fe II emission strongly aspect-dependent.

We consider the former of these two models for the Mg II BALQSOs the more likely possibility, but much more extensive data in both the IR and optical are required.

This work was supported in part by National Science Foundation grants AST 86-20427, AST 87-00741, AST-9001181, and AST-9005117, which are gratefully acknowledged, as is Scott Anderson's participation in the earlier phases of this project. We thank P. Barthel, T. Boroson, R. Carswell, R. Cutri, F. Hamann, and J. Surdej for useful conversations. P. C. H. is grateful to the Royal Society for a Fellowship. R. J. W. extends personal thanks to many friends for their support during a difficult period.

APPENDIX A

DEFINITION OF THE BALNICITY INDEX

We provide here the procedure used to measure the balnicity index.

1. Define a continuum as sensibly as possible between the rest wavelengths of the Si IV and C IV emission features. So far we have not been able to automate this procedure in an entirely satisfactory manner.
2. Define the rest system of the QSO in the following way: (*a*) Measure the peak of the Mg II line whenever possible. (*b*) If Mg II is not available, use the C III] peak. (*c*) If C III] is not available, use the peak of the C IV emission, provided that it does not appear to be badly distorted by absorption. When the nature of the systematic shifts between Mg II, C III], and C IV is better understood (see § 4), it may be desirable to introduce velocity offsets when the C III] or C IV peaks must be measured.
3. Interpolate over any absorption features which are identified with species other than C IV.
4. Evaluate the following integral, which is a modified equivalent width (expressed in km s^{-1})

$$\mathrm{BI} = -\int_{25{,}000}^{3000} [1 - f(V)/0.9] C \, dV \ ,$$

where $f(V)$ is the normalized flux as a function of velocity displacement from the line center. The value of C is initially set to zero. It is set to 1.0 whenever the quantity in brackets has been continuously positive over an interval of 2000 km s^{-1}. It is reset to zero whenever the quantity in brackets becomes negative. Thus, the first 2000 km s^{-1} of any swath of contiguous absorption does not contribute to the balnicity index. An object which had two deep troughs, one of width 1990 km s^{-1} and the other of width 2010 km s^{-1}, would have a balnicity index of 10. The balnicity index thus measures the equivalent width (in km s^{-1}) of those portions of contiguous absorption exceeding 2000 km s^{-1}, but only counts as "absorption" features dipping 10% or more below the estimated continuum. The minimum value of the index is therefore zero, and, since the maximum value of the quantity in square brackets is 1.0, and the upper limit of the integral is 3000 km s^{-1} to the blue of the C IV line center, a completely black trough covering the region from 25,000 km s^{-1} blueward of the C IV line center to the C IV line center would have the maximum possible value of the balnicity index, namely, 20,000 km s^{-1}.

The rationale for the requirement of having the residual intensity drop 10% below the continuum before any contribution to the balnicity index can be made is to avoid getting a nonzero index from non–BALQSOs in cases in which the continuum has been drawn too high, and 10% seems a reasonable margin of safety. Of course any "true" BALQSO which had broad but very shallow absorption would be missed. An object which illustrates such a borderline case is UM 660, illustrated in Turnshek (1988). The contiguity condition is imposed to avoid mistaking absorption complexes arising from cosmologically intervening material for material associated with the QSO. A value of 2000 km s^{-1} appears to be a reasonable cutoff for such complexes, though more extensive complexes may exist. We have cited some examples in § 3.

The 25,000 km s^{-1} blue limit on the integral is chosen to avoid ambiguities associated with the Si IV emission and absorption, while the 3000 km s^{-1} red limit is set to avoid inclusion of objects with strong absorption complexes of C IV occurring at or very near the emission-line redshift. The object 0302+170 mentioned in § 3 is an example of an object which has a balnicity index of zero by virtue of the 3000 km s^{-1} limit. Finally, note that the velocities appearing in the definition of the balnicity index ignore the C IV doublet splitting of about 550 km s^{-1} and are measured as if the transition were a singlet with wavelength 1549.0 Å.

A FORTRAN code for computing the balnicity index is available.

APPENDIX B

THE DETACHMENT INDEX

As discussed in § 4, we wish to define a "detachment index" for each object in order to test the reality of certain suspected correlations involving objects whose C IV absorption troughs are detached from the C IV emission line. Since most of the troughs set

in rather abruptly on the low-velocity side, it is not too difficult to define an "onset velocity." However, it is not simply the velocity at which the absorption commences but rather this velocity relative to the width of the emission which determines one's subjective impression of whether a trough is detached or not.

In practice, there are a number of ambiguities about how to proceed. The most serious of these involve the cases where there are multiple or complex troughs. A separate detachment index for each trough can be calculated, and it is not obvious which of these indices should be used in checking for correlations. Some troughs are clearly single (e.g., 1333+2840), while others are clearly multiple (e.g., 0043+0048), but in many other cases it is not clear when and how to divide the absorption into multiple troughs. We have dealt with the first of these ambiguities by running two sets of correlation tests. In one set we used the detachment index of the lowest velocity trough, and in the second set we used the detachment index associated with the strongest trough (with "strength" as defined below). We found that the best evidence for correlations appeared when we chose the latter of these two possibilities.

The following procedure for defining the existence of one or more troughs in each object and for assigning a detachment index to each trough is arbitrary, but the indices assigned seem in accord with subjective impressions of "detachment."

1. As in the case of the balnicity index, we must define a continuum in the region of the Si IV and C IV lines.

2. Half-Gaussians are fitted to the blue and red sides of the C IV emission peaks, with separate half-width at half-maximum parameters on the blue and red sides. With a few exceptions, the fit to the red side is acceptable down to about 30% or 40% of the peak height to the red of which the fit underestimates the flux. The fit to the blue side is obviously much more difficult and uncertain because of the absorption trough. The fit to the blue side is required because at low velocities the effective continuum seen by the absorption trough includes the C IV line emission.

3. As in the computation of the balnicity index, every occurrence of a contiguous stretch of 2000 km s^{-1} in which the residual intensity was below 90% of the effective continuum was considered an "isolated trough." In contrast to the balnicity index, however, the region of velocity space from 0 to 3000 km s^{-1} was not excluded, since we are dealing with objects which are already established as bona fide BALQSOs by virtue of a positive balnicity index, and since for the purpose of measuring the detachment index the region from 0 to 3000 km s^{-1} is of interest.

4. In many cases these isolated troughs have such strong structure within them that, although the residual intensity within the trough never rises above the 90% threshold, we should consider them to consist of several separate troughs. We used the following algorithm to decide when and how to divide the large isolated troughs into separate troughs: (*a*) Locate all the "strong" local minima of the residual intensity within a given isolated trough. "Strong" minima are minima which are bracketed by local maxima which rise at least 0.125 above these minima. (*b*) If these strong minima are separated from their neighbors by 3000 km s^{-1} or more, they define separate troughs.

5. As in the calculation of the balnicity index, we compute the strength of each trough by measuring its equivalent width (in km s^{-1}) relative to a level at 90% of the effective continuum. For troughs formed by strong structure within the large isolated troughs as described in paragraph 4 above, the boundaries for these troughs are taken to be the maxima which separate the trough minima.

6. For each trough we define the "onset velocity" for that trough by the point where the residual intensity falls from the maximum redward of the trough minimum to a point which is the average of that maximum and the trough minimum. (For the first minimum which is encountered after the residual intensity falls below 0.90, the "maximum" is taken to be the 0.90 intensity point. In instances where noise or small real fluctuations cause the residual intensity to cross this average more than once, we take the average velocity of these crossings.)

7. For each trough its detachment index is the onset velocity of that trough divided by a measure of the emission width. Ideally, we should use the FWHM of the C IV emission, but, as noted above the half–half-width on the blue side is extremely difficult to estimate. Even the red side is sometimes apparently eaten into. We therefore used a mean of the C IV red-side widths and the widths of the C III] line after deblending the Al III. For reasons discussed in § 3 the C III] half–half-widths are substantially larger than the C IV red-side half–half-widths. Before calculating the emission width to be used in the evaluation of the detachment index, we therefore scaled down the C III] widths so that in the mean the C IV and C III] widths agreed. To the reader who has followed this tortuous description to the bitter end, we emphasize that this seeming bit of hocus-pocus is simply to provide a sensible and moderately stable estimate for the emission width which is used to compute the detachment index. While complex to describe, the algorithm for the computation of the detachment index is simple to program and relatively objective.

APPENDIX C

INTERVENING ABSORPTION SYSTEMS

The set of spectra presented in this paper were obtained for the purpose of investigating emission-line and continuum properties. However, a number of strong intervening low-ionization absorption systems were noted. For observers who may be interested in obtaining higher resolution and higher signal-to-noise observations of some of these systems, we provide a list in Table 7, with approximate redshifts and brief comments. Except where noted, the reality and identification of all systems appear to be "certain" in the sense of having strong Mg II doublets. However, we caution that the list is *not* intended to be complete and *should not* be used for statistical purposes without further analysis.

TABLE 7

LIST OF INTERVENING ABSORPTION SYSTEMS

Object	Redshift	Comments
0006+0230.....	1.701	Mg I, Fe II, Al II
0009−0138.....	1.386	Fe II, Al III
0013−0029.....	1.971	Mg I, Fe II, Al II, Si II, C II, O I
0019+0107.....	1.828	
0146+0142.....	1.686	Fe II
	1.282	
	1.128	(Blue of C IV)
0903+1734.....	1.616	Mg I:
	1.541	Fe II; possible lines at 6804.8, 6828.7 Å unidentified
1011+0906.....	1.491	Mg I, Fe II
	1.459	Possible weak Mg II; system uncertain
1131+0114.....	1.785	Fe II
1139−0139.....	1.484	Mg I, Fe II, Al III, Al II, Si II; Si II λ1808 appears to be present in this very strong system
	1.152	Fe II
1146+0207.....	1.395	Mg I:, Fe II, Al II:
1208+1535.....	1.588	Fe II
	1.226	Fe II
1215+1527.....	1.445	
1234+0122.....	1.334	Mg I, Fe II, Al III, Al II; the 1854 Å line of Al III from this system confuses the measurement of the balnicity index in this marginal BALQSO
	1.304	Mg I, Fe II
1239+0955.....	1.659	Fe II
1242+0006.....	1.824	Fe II, Al II; Al II line in blue wing of C IV emission
1328+0223.....	1.218	Probable Mg II; system uncertain
1331−0108.....	1.426	Fe II
	0.656	Mg I
1413+1143.....	1.659	Mg I would be obscured by A band; Fe II, Al III
1428+0202.....	1.241	Mg I, Fe II, Al III
1429−0053.....	1.512	Fe II, Al III, Al II
1433+0223.....	1.216	Probable Mg II, possible Fe II; system uncertain
1439+0047.....	1.280	Fe II, Al II, Al III, Si II; λ1808 Si II present
2230+0232.....	1.863	Mg I, Fe II, Al III:, Al II, Si II, C II
	1.058	Fe II
2350−0045.....	1.247	Fe II
	1.032	Fe II
2351+0120.....	0.940	Fe II

REFERENCES

Antonucci, R. R. J., & Miller, J. S. 1985, ApJ, 297, 621
Baldwin, J. A., Wampler, E. J., & Gaskell, C. M. 1989, ApJ, 338, 630
Barthel, P. 1990, private communication
Boroson, T. A., Persson, S. E., & Oke, J. B. 1985, ApJ, 293, 120
Boyd, R. N., & Ferland, G. J. 1987, ApJ, 318, L21
Braun, E., & Milgrom, M. 1989, ApJ, 342, 100
Corbin, M. R. 1990a, ApJ, 357, 346
———. 1990b, private communication
Cowley, A. P., & Crampton, D. 1987, AJ, 94, 16
Cutri, R. M. 1990, private communication
Espey, B. R., Carswell, R. F., Bailey, J. A., Smith, M. G., & Ward, M. J. 1989, ApJ, 342, 666
Foltz, C. B., Chaffee, F. H., Jr., Hewett, P. C., MacAlpine, G. M., Turnshek, D. A., Weymann, R. J., & Anderson, S. A. 1987, AJ, 94, 1423
Foltz, C. B., Chaffee, F. H., Jr., Hewett, P. C., Weymann, R. J., Anderson, S. A., & MacAlpine, G. M. 1989, AJ, 98, 1959
Foltz, C. B., Chaffee, F. H., Hewett, P. C., Weymann, R. J., & Morris, S. L. 1990, BAAS, 2, 806
Foltz, C. B., Weymann, R. J., Hazard, C., & Turnshek, D. A. 1985, BAAS, 16, 1006
Foltz, C. B., Weymann, R. J., Peterson, B. P., Sun, L., Malkan, M. A., & Chaffee, F. H., Jr. 1986, ApJ, 307, 504
Francis, P. J., Hewett, P. C., Foltz, C. B., Chaffee, F. H., Weymann, R. J., & Morris, S. L. 1991, ApJ, in press
Gaskell, C. M. 1982, ApJ, 263, 79
Hamann, F., Morris, S. L., & Weymann, R. J. 1990, in preparation
Hartig, G. F., & Baldwin, J. A. 1986, ApJ, 302, 64 (HB)
Hazard, C. 1989, remark made following colloquium given by R. Weymann, Cambridge, England, 1989 July
Hazard, C., McMahon, R., Webb, J. K., & Morton, D. C. 1987, ApJ, 323, 263
Hazard, C., Morton, D. C. Terlevich, R., & McMahon, R. 1984, ApJ, 282, 33
Hewett, P. C., Francis, P. J., Chaffee, F. H., Jr., Foltz, C. B., Morris, S. L., & Weymann, R. J. 1990, in preparation
Jakobsen, P., Perryman, M. A. C., Ulrich, M. H., Macchetto, F., & di Serego Alighieri, S. 1986, ApJ, 303, L27
Joly, M. 1988, in Physics of Formation of Fe II Lines outside LTE, ed. R. Viotti, A. Vittone, & M. Freidjung (Dordrecht: Reidel)
Junkkarinen, V. 1983, ApJ, 265, 73
———. 1989, in IAU Symposium 134, Active Galactic Nuclei, ed. D. E. Osterbrock & J. S. Miller (Dordrecht: Kluwer)
Junkkarinen, V. T., Burbidge, E. M., & Smith, H. E. 1983, ApJ, 265, 51
———. 1987, ApJ, 317, 460 (JBS)
Kellermann, K. I., Sramek, R., Schmidt, M., Shaffer, D. B., & Green, R. 1989, AJ, 98, 1195
Low, F. J., Cutri, R. M., Kleinmann, S. G., & Huchra, J. P. 1989, ApJ, 340, L1
Malkan, M., Rieke, M., & Weymann, R. J. 1985, unpublished
Morris, S. L. 1988, ApJ, 330, L83
Morris, S. L., Weymann, R. J., Foltz, C. B., Turnshek, D. A., Shectman, S., Price, C., & Boroson, T. A. 1986, ApJ, 310, 40
Netzer, H. 1988, in Physics of Formation of Fe II Lines outside LTE, ed. R. Viotti, A. Vittone, & M. Freidjung (Dordrecht: Reidel)
Oke, J. B., & Gunn, J. E. 1982, PASP, 94, 586
Press, W. H., Flannery, B. P., Teukolsky, S. A., & Vetterling, W. T. 1986, Numerical Recipes: The Art of Scientific Computing (Cambridge: Cambridge Univ. Press)
Sargent, W. L. W. 1988, in STScI Symposium Series 2, QSO Absorption Lines: Probing the Universe, ed. J. C. Blades, D. Turnshek, & C. Norman (Cambridge: Cambridge Univ. Press)
Schmidt, G. D., Weymann, R. J., & Foltz, C. B. 1989, PASP, 101, 713
Steiner, J. E. 1981, ApJ, 250, 469

Stocke, J., Foltz, C. B., Morris, S. L., & Weymann, R. J. 1990, in preparation
Surdej, J., & Hutsemekers, D. 1987, A&A, 177, 42
Turnshek, D. A. 1984a, ApJ, 278, L87
———. 1984b, ApJ, 280, 51
———. 1988, in STScI Symposium Series 2, QSO Absorption Lines: Probing the Universe, ed. J. C. Blades, D. Turnshek, & C. Norman (Cambridge: Cambridge Univ. Press)
Turnshek, D. A., Foltz, C. B., Grillmair, C. J., & Weymann, R. J. 1988, ApJ, 325, 651
Uomoto, A. 1984, ApJ, 284, 497
Visnovsky, K., Impey, C. D., Foltz, C. B., Hewett, P. C., & Weymann, R. J. 1990, in preparation
Weymann, R. J., Carswell, R. F., & Smith, M. G. 1981, ARA&A, 19, 41
Weymann, R. J., Morris, S. L., & Anderson, S. A. 1988, in Proc. Georgia State University Conf. on Active Galactic Nuclei, ed. P. J. Wiita & H. R. Miller (Berlin: Springer-Verlag)
Wilkes, B. J., & Carswell, R. F. 1982, MNRAS, 201, 6
Wills, B. 1988, in Physics of Formation of Fe II Lines outside LTE, ed. R. Viotti, A. Vittone, & M. Freidjung (Dordrecht: Reidel)

Note added in proof.—In Table 1, UM 253 is 0029+0017, not 0025−0151, and the coordinate designations for three objects in Table 1 and Figure 1 should be changed to 1011+0906, 1303+3048, and 1309−0536.